The influence of heavy metal stress on the evolutionary transition of teosinte to maize

Jonathan Acosta-Bayona[1], Miguel Vallebueno-Estrada[2], and Jean-Philippe Vielle-Calzada[1]*

[1]Grupo de Desarrollo Reproductivo y Apomixis, Unidad de Genómica Avanzada Langebio, Centro de Investigación y de Estudios Avanzados del IPN, Km 9.6 Libramiento Norte Carretera Irapuato-León, CP36825 Irapuato Guanajuato, México

[2]Swedish University of Agricultural Sciences, Umeå, Sweden

*Author for correspondence:
Jean-Philippe Vielle-Calzada
Tel: 421663000 ext. 3100
Email: vielle@cinvestav.mx

ORCIDs
Acosta-Bayona: https://orcid.org/0009-0005-7305-6245
Vallebueno-Estrada: https://orcid.org/0000-0001-8647-8758
Vielle-Calzada: https://orcid.org/0000-0002-3017-2490

Summary

Maize originated from teosinte *parviglumis* following a subspeciation event occurred in volcanic regions of Mesoamerica. The elucidation of the phenotypic changes that gave rise to maize have focused on the direct consequences of domestication, with no insights on how environmental factors could have influenced specific gene function and human selection. We explored the impact of heavy metal (HM) stress by exposing both subspecies to sublethal concentrations of copper and cadmium. We also assessed the genetic diversity of loci encompassing three HM response genes affected by domestication: *ZmHMA1*, *ZmHMA7* – encoding for heavy metal ATPases of the $P1_b$ family-, and *ZmSKUs5,* encoding a multicopper oxidase. *ZmHMA1* and *ZmSKUs5* map in the short arm of chromosome five, in a genomic region containing multiple linked QTLs with pleiotropic effects on domestication. A genomic analysis of the full chromosome shows that their loci show strong positive selection as compared to previously identified domestication genes. Exposure of teosinte *parviglumis* to HM stress results in a plant architecture reminiscent of extant maize, and upregulation of *Teosinte branched1* (*Tb1*) in the meristem. *ZmHMA1* and *ZmHMA7* are expressed throughout development and respond to HM stress in both subspecies. *ZmHMA1* is mainly involved in restricting plant height and optimizing the number of female inflorescences and seminal roots. Our results suggest that HM stress acted on specific ATPases involved in homeostasis, giving rise to phenotypic variants that were identified and selected by humans during domestication.

Key words: maize, teosinte *parviglumis*, heavy metals, domestication, ATPases, seminal roots.

Introduction.

Driven by either conscious or unconscious human selection, domestication can be considered a gradual evolutionary process resulting in the adaptation to agroecological environments and anthropogenic preferences (Ross-Ibarra et al. 2007). In the case of plants, the obvious consequences of domestication are represented by visually recognizable traits that include changes in photoperiod response, reduced capacity of seed dispersion, reduced lateral branching, larger fruits or grains, reduced duration of seed dormancy, and increase in the size of female inflorescences (Pickersgill 2007; Larson et al. 2014). Notably, research efforts to understand the phenotypic changes that gave rise to maize have mainly focused on the direct consequences of domestication in aerial organs and sometimes roots (Chen et al. 2022; Lopez-Valdivia et al. 2022; Ren et al. 2022), with no emphasis on the role of adaptive environmental responses that, by acting on specific gene function, could have given rise to phenotypic traits that were identified and selected by humans.

It is generally accepted that domestication of maize (*Zea mays* ssp. *mays*) from teosinte *parviglumis* (*Zea mays* ssp. *parviglumis*) initiated in Mesoamerica around 9,000 years before present (Matsuoka et al. 2002). The initial evolutionary transition that resulted in the event of subspeciation most likely occurred within the Balsas river drainage, in regions geographically converging with the Trans-Mexican Volcanic Belt, at the intersection of the States of Mexico, Guerrero, and Michoacan (Matsuoka et al. 2002). Although the nature of the initial phenotypic changes that allowed the emergence of primitive maize remains unclear, the most obvious architectural and morphological differences between both subspecies affect their vegetative and reproductive organs. Teosinte *parviglumis* generates numerous lateral branches ending in male inflorescences, while maize often has a few short or no lateral branches, not ending in male reproductive organs (Wills et al. 2013). Additionally, the seeds of teosinte *parviglumis* are covered by a hard glume that protects the kernel externally, while in maize glumes are reduced, soft and do not cover the kernel (Doebley and Stec 1993). Large scale efforts involving physical mapping and comparative genomic analysis have resulted in the identification of numerous regions showing differential nucleotide variability between teosinte *parviglumis* and the B73 reference

86 maize genome. In some cases, mutations in genes located within those genomic regions
87 result in phenotypes that reveal their involvement in domestication traits. One of the major
88 genes affected by maize domestication is *Teosinte branched1* (*Tb1*), a transcription factor
89 of the TCP family that controls lateral branching, sexual determination, and glume
90 formation (Doebley et al. 1997; Martín-Trillo and Cubas 2010). *Tb1* acts as a repressor of
91 lateral branching (Studer et al. 2017), giving rise to maize plants usually composed of a
92 single stem. Other genes involved in domestication include *Teosinte glume architecture1*
93 *(Tga1)*, *ramosa2 (ra2)* and *Zea floricaula leafy2 (zfl2),* among others (Bomblies and
94 Doebley 2006; Sigmon and Vollbrecht 2010; Wang et al. 2015).
95
96 The importance of phenotypic plasticity is considered as likely relevant in the
97 domestication history of crops (Ross-Ibarra et al. 2007; Lorant et al. 2020; Mueller et al.,
98 2023); however, the role of environmental factors influencing their origins remains elusive
99 and poorly investigated. A previous study showed that teosinte *parviglumis* grown under
100 low temperatures and CO_2 concentrations - reminiscent of those prevailing in the late
101 Pleistocene and early Holocene - exhibit some phenotypes related to the domestication
102 syndrome, including short branches, a single main stalk, and partially open seed fruitcases
103 (Piperno et al. 2015; Piperno et al. 2019); however, the genetic basis of these changes have
104 not been investigated. Although these results suggest that phenotypic plasticity could have
105 influenced the domestication process, to this date there are no hints on how the adaptation
106 to local environmental conditions could have affected specific gene function and guided
107 human selection.
108
109 Recent genomic evidence indicates that admixture of maize with native teosinte *mexicana*
110 populations (*Zea mays* ssp. *mexicana*) contributed to maize adaptation across a wide range
111 of altitudes and latitudes in the American continent (Yang et al. 2023); however, the earliest
112 maize macro-specimens found to date lack teosinte *mexicana* admixture and exhibit
113 morphological attributes of fully domesticated cobs, indicating that *mexicana* is not a direct
114 ancestor of maize and that its introgression occurred after initial divergence from teosinte
115 *parviglumis* (Vallebueno-Estrada et al. 2023; Acosta-Bayona et al. 2024). Consequently,
116 the nature of the genetic factors that guided the emergence of maize remain largely

117 unknown, and the initial phenotypic changes that caused the original divergence of these
118 two subspecies have not been identified. It is also unknown if domestication initiated by
119 direct action of human selection on teosinte natural standing variation, or if the response to
120 specific environmental factors generated phenotypic changes that were identified and
121 selected by humans to act on native teosinte *parviglumis* populations.
122
123 Maize can adapt to abiotic factors such as heavy metal (HM) stress through numerous
124 mechanisms that prevail during development (AbdElgawad et al. 2020; Gallo-Franco et
125 al. 2020; Malenica et al. 2021; Gao et al. 2022). These include metal immobilization by
126 mycorrhizal association, metal sequestration, or complexation by exuding organic
127 compounds from roots, metal intracellular sequestration and compartmentalization in
128 vacuoles. HMs include essential elements that are necessary for maize growth through
129 enzymatic function, such as iron (Fe), manganese (Mn), zinc (Zn), magnesium (Mg),
130 molybdenum (Mo), and copper (Cu); and non-essential elements like Cadmium (Cd),
131 chromium (Cr), lead (Pb), aluminum (Al), and selenium (Se). In general, HM stress leads
132 to visibly reduced plant growth due to the reduced cell elongation and cell wall elasticity.
133 At the molecular level, metal toxicity can disturb the cellular redox balance and lead
134 directly or indirectly to oxidative stress and the formation of reactive oxygen species
135 (ROS), shifting the redox balance to the pro-oxidative side until the antioxidative defense
136 system allows a new balanced redox status (Smeets et al. 2009; Hall 2002).
137
138 The comparison of the *Palomero toluqueño* and B73 genomes resulted in the identification
139 of a large collection of identical sequence regions (IdSRs) with low nucleotide variability
140 and transcriptional evidence of expression (Vielle-Calzada et al. 2009). Putative
141 domestication loci included *ZmHMA1* and *ZmHMA7*, two genes encoding members of the
142 $P1_b$-ATPases protein superfamily, also known as Heavy Metal ATPases (P-type ATPases)
143 characterized by the generation of a phosphorylated intermediate during the transport
144 reaction cycle. Members of this superfamily contain 8 to 12 transmembrane domains as
145 well as conserved ATP binding, phosphorylation and dephosphorylation sites (Solioz and
146 Vulpe 1996; Axelsen and Palmgren 2001; Voskoboinik et al. 2003; Williams and Mills
147 2005). The superfamily can be divided in subfamilies that include H±ATPases (type 3_A) in

148 plants and fungi, Na+/K ATPases (type $2_{C/D}$) in animals, Ca2±ATPases (type $2_{A/B}$), and
149 heavy metal (HM) transporting ATPases (type 1_B) capable of transporting a large variety
150 of HM cations across cell membranes. *ZmHMA1* and *ZmHMA7* are type 1_B ATPases that
151 include a conserved Cys-Pro-Cys/His/Ser motif within a transmembrane domain necessary
152 for the translocation of HMs cations through the membrane channel. A third *Palomero*
153 *toluqueño*/B73 IdSR included *Skewed Root Growth Similar5* (*ZmSKUs5*), a gene encoding
154 a Skewed5 (SKU5)-similar (SKS) protein classified as a multi-copper oxidase containing
155 cuperdoxin domains (Sedbrook et al. 2002). All three genes map to chromosome five
156 (chr.5), with *ZmHMA1* and ZmSKUs*5* within a genomic region that fractionates into
157 multiple QTLs under selection during the *parviglumis* to maize transition (Doebley and
158 Stec 1993; Lemmon and Doebley, 2014). Contrary to major domestication loci showing a
159 single highly pleiotropic gene responsible for important domestication traits, in this chr.5
160 genomic region the smallest 1.5-LOD support interval contained more than 50 genes,
161 suggesting that phenotypic effects are due to multiple linked QTLs (Lemmon and Doebley,
162 2014). While the functional characterization of all three maize genes remains elusive, the
163 Arabidopsis and barley *ZmHMA1* homologs act during heavy metal transport in the
164 chloroplast (Boutigny et al. 2014), demonstrating their functional involvement in
165 homeostasis.
166
167 To investigate a possible involvement of heavy metal response in the origin and
168 domestication of maize, we compared the phenotypic changes that teosinte *parviglumis*
169 and maize undergo when grown in the presence of sublethal concentrations of Cu and Cd.
170 We show that teosinte *parviglumis* responds to HM stress by acquiring an aerial
171 architecture reminiscent of extant maize, and that *Tb1* expression is upregulated in teosinte
172 *parviglumis* meristems when grown under HM stress. A large-scale genomic analysis of
173 nucleotide variability across maize chr.5 indicates that loci encompassing *ZmHMA1*,
174 *ZmHMA7*, and *ZmSKUs5* show reduced nucleotide variability in maize as compared to
175 teosinte *parviglumis*. Both *ZmHMA1* and *ZmHMA7* are active throughout maize and
176 teosinte *parviglumis* development, and their expression responds to HM stress. In addition,
177 mutations in *ZmHMA1* show phenotypic defects related to the maize domestication
178 syndrome, some of which are only manifested under exposure to HMs. Overall, our results

179 indicate that the evolutionary transition that gave rise to extant maize was influenced by
180 heavy metal stress through the activity of P1b-ATPases.
181

182 ## Results

183

184 ***Teosinte parviglumis responds to heavy metal stress by acquiring an architecture***
185 ***reminiscent of extant maize.***

186

187 To compare HM response in teosinte *parviglumis* and maize, we exposed wild-type W22
188 maize inbred and CIMMYTMA 29791 teosinte *parviglumis* individuals to sublethal
189 concentrations of Cu (400 mg/kg of $CuSO_4$) and Cd (16mg/kg of $CdCl_2$). $CuSO_4$ and $CdCl_2$
190 were homogenized in soil before transplant and grown under controlled greenhouse
191 conditions. HM concentrations were based on preliminary dose responses that allowed
192 maize plants to reach reproductive stages and complete their life cycle (AbdElgawad et al.
193 2020). As previously reported (Atta et al. 2023), maize individuals grown in the presence
194 of HMs showed a significant reduction in aerial traits such as stem diameter, size of leaves,
195 size and number of roots, and size of female inflorescences (Figure 1; Tables 2 and S2).
196 On average, stem diameter showed a reduction of about 17% as compared to plants grown
197 in absence of HM stress (Figure 1f to 1j). Similarly, the length and width of developing
198 leaves showed average reductions of 12%, and mature leaves of 6%. Reproductive traits
199 such as the number of female inflorescences (NFI) and their average weight (WFI) showed
200 a significant reduction (NFI = 1.20 ± 0.42 in absence of HMs and NFI = 0.70 ± 0.67 in
201 presence of HMs; WFI = 40.06 ± 14.39 in absence of HMs and WFI = 37.75 ± 18.83 in
202 presence of HMs; Table 2). As expected, the most significant effects occurred in the root
203 system, with a significant increase in the number of brace roots under HMs (NBR = 12.90
204 ± 4.33 in absence of HMs; NBR = 16.30 ± 4.99 in presence of HMs; Table 2), and a
205 significant decrease in their length (LBR = 16.15 ± 9.75 cm in absence of HMs; LBR =
206 4.00 ± 2.04 cm in presence of HMs; Table 2). The number and length of crown roots were
207 reduced on average by 33% and 18%, respectively (NCR = 11.30 ± 2.11 in absence of
208 HMs; NCR = 7.60 ± 0.97 in presence of HMs; LCR = 58.90 ± 21.87 cm in absence of
209 HMs; LCR = 48.85 ± 11.80 cm in presence of HMs; Table 2). Nodal roots also showed a

210 significant reduction in their number and length (NNR = 10.50 ± 2.27 in absence of HMs;
211 NNR = 6.70 ± 2.79 in presence of HMs; LNR = 87.20 ± 16.80 cm in absence of HMs; LNR
212 = 55.30 ± 21.10 cm in presence of HMs; Tables 2 and S2). By contrast, the number (NSR)
213 and length (LSR) of seminal roots was significantly increased in the presence of HMs (NSR
214 = 4.10 ± 1.45 in absence of HMs; NSR = 6.60 ± 1.35 in presence of HMs; LSR = 27.70 ±
215 13.38 cm in absence of HMs; LSR = 43.50 ± 14.01 cm in presence of HMs) when measured
216 50 days after transplant (Table 2).
217
218 Interestingly, teosinte *parviglumis* exhibited a maize-like phenotype when grown in the
219 presence of HMs, with complete absence of tillering in most plants (Figure 1; Tables 1, S1
220 and S3). From a total of 30 plants tested, 28 showed total absence of tillering, and two
221 initiated secondary stems during vegetative stages but arrested their growth early during
222 development, resulting in the presence of a single dominant stem at reproductive stages
223 (Figure 1a to 1d). Additionally, all 30 plants tested showed complete absence or residual
224 lateral branching, with unusual proliferation of female inflorescences arising from
225 independent axillary meristems in primary stems (Figure 1e). This significant increase in
226 the number of female inflorescences clustered within a single stem (NFI = 1.80 ± 0.63 in
227 absence of HMs; NFI = 3.90 ± 1.66 in presence of HMs; Figure 1e and Table 1) was
228 associated with shorter flowering time as compared with normal growing conditions in
229 absence of HMs (Figure 1d). In addition, teosinte *parviglumis* grown in the presence of
230 HMs showed significantly reduced leaf length (LIL = 71.30 ± 11.32 cm in absence of HMs;
231 56.25 ± 7.80 cm in presence of HMs; Table 1). The absence of lateral branches resulted in
232 lower values of aerial dry weight (DWAP = 133.49 ± 28.28 gr in the absence of HMs;
233 DWAP = 82.72 ± 11.67 gr in presence of HMs; Table 1). Teosinte *parviglumis* grown
234 under HMs showed a significant reduction in the length of brace roots (LBR = 20.00 ±
235 11.49 cm in absence of HMs; LBR = 2.88 ± 0.66 cm in presence of HMs; Table 1), but no
236 significant changes in their number. The number and length of crown and nodal roots was
237 not affected by HM stress, nor did the presence of HMs modify the absence of seminal
238 roots intrinsic to teosinte *parviglumis* accessions (Perkins and Lynch 2021). Taken
239 together, these results suggest that the response of maize and teosinte *parviglumis* to HM

240 stress can give rise to phenotypes previously shown to distinguish both subspecies at the
241 light of the domestication syndrome.
242
243
244 ***Genomic regions encompassing ZmHMA1, ZmHMA7 and ZmSKUs5 show reduced***
245 ***nucleotide variability in extant maize as compared to teosinte parviglumis.***
246
247 *ZmHMA1* and *ZmSKU5* mapped 52.1 and 41.8 cM, respectively, in a genetic map of chr.5
248 calculated to be 86.64 cM, with an average megabase pair to centimorgan ratio of 1.873
249 Mbp/cM (Lemmon and Doebley, 2014; Figure S1). The corresponding mapping population
250 used isogenic recombinant inbred lines (NIRILs) with informative cross-over events
251 concentrated in the region of interest and replicated phenotypic assessments in block
252 experiments. Multiple QTLs were detected in a region spanning across 82 cM, none with
253 single large effect genes such as those found in other chromosomes (Wang et al., 2005;
254 Studer et al. 2011; Wills et al., 2013), suggesting that several associated domestication
255 traits are due to multiple linked QTLs of small effect (Lemmon and Doebley, 2014). The
256 location of *ZmSKU5* overlaps with a single wide 1.5-LOD support interval that spreads
257 across 50.6 cM (number of kernels per rank; Figure S1). By contrast, *ZmHMA1* overlaps
258 with a contiguous region containing no less than five QTL 1.5- LOD support intervals (ear
259 diameter; number of kernels per rank; percentage of staminate spikelets; tassel branch
260 number; and tillering index; Figure S1).
261
262 To determine if the regulatory and coding regions of *ZmHMA1, ZmHMA7,* and *ZmSKUs5*
263 were affected by human selection, we calculated their level of nucleotide variability based
264 on single nucleotide polymorphisms (SNPs) for all extant maize and teosinte *parviglumis*
265 accessions included in the diversity panel HapMap3, using the corresponding sequences of
266 *Tripsacum dactyloides* as an outgroup. The levels of the nucleotide variability index - $\pi(m)$
267 and $\pi(t)$ for maize and teosinte *parviglumis*, respectively - were determined in bins of 100
268 nt using VCFtools, including alignments encompassing a genomic region that included 15
269 kb upstream of the START codon, the corresponding coding region for each gene, and 15
270 kb downstream of the STOP codon (Figure 2 and Table S4). In the case of *ZmHMA1*, the

271 upstream region values were π(m)= 0.00071 and π(t)= 0.00870, and for the downstream
272 region, π(m)=0.00097 and π(t)=0.00248. By contrast, the *ZmHMA1* coding sequence
273 showed low values in both subspecies: π(m)= 0.0050 and π(t)= 0.00106. These results
274 indicate that human selection in the *ZmHMA1* locus preferentially affected its upstream
275 and downstream regulatory regions (Figure 2a and Table S4). Interestingly, although maize
276 π values are at least one order of magnitude lower than π values in teosinte, π(t) values are
277 also one order of magnitude lower than π values of *Tripsacum sp*., suggesting that a genetic
278 bottleneck also affected teosinte *parviglumis* in these loci. *ZmHMA7* showed contrasting
279 values of π(m) and π(t) across the entire coding sequence and its regulatory regions (Figure
280 2b). For the upstream region, values were π(m)= 0.0009 and π(t)=0.00411; for the
281 *ZmHMA7* coding region, π(m)= 0.00015 and π(t)= 0.00148; and for the downstream region,
282 π(m)=0.00066 and π(t)=0.00454. *ZmSKUs5* also showed contrasting nucleotide variability
283 in the entire coding and flanking regions (Figure 2c and Table S4). Values were π(m)=
284 0.0011 and π(t)= 0.00735 for the upstream region, π(m)= 0.00044 and π(t)= 0.00754 for
285 the coding sequence, and π(m)=0.00203 and π(t)=0.00626 for the downstream region
286 (Table S4). For all three genes, similar π values in the coding region of maize landraces
287 and improved lines indicates that the loss of nucleotide variability occurred during the
288 teosinte *parviglumis* to maize transition, and not during subsequent contemporary breeding
289 (Table S4). By contrast, the *ZmGLB*1 neutral control locus shows equivalent levels of
290 nucleotide variability in maize and teosinte *parviglumis* (Eyre-Walker et al. 1998).
291
292 We also compared the level of genetic variability in *ZmHMA1*, *ZmSKUs5*, and *ZmHMA7*
293 (and their neighboring regions) to all chr.5 genes categorized as likely affected by
294 domestication (Hufford et al., 2012), and to the full collection of neutral genes distributed
295 across the whole chromosome. The analysis was conducted using 100 bp bins and sliding
296 windows of 50 bp; for a total of 385,829 bins in the case of chr.5 domestication genes, and
297 2,373,010 bins for neutral genes. As shown in Figure S2, the levels of nucleotide variability in
298 the three candidate genes and their six neighboring loci are significantly reduced in maize
299 landraces as compared to teosinte *parviglumis* inbred lines. When compared to the full neutral
300 gene set of chr.5, this reduction is more severe than the reduction affecting 304 previously
301 identified domestication genes, confirming the exceptional selective pressure that was imposed

302 in those three loci during the evolutionary transition from teosinte *parviglumis* to extant
303 maize.
304
305
306 ***ZmHMA1 and ZmHMA7 are active throughout development and their expression is***
307 ***influenced by the presence of heavy metals.***
308
309 The gene structure of *ZmHMA1, ZmHMA7,* and *ZmSKUs5* is shown in Figure 3. The coding
310 sequence of *ZmHMA1* and *ZmHMA7* is approximately 21.6 Kb and 4.5 Kb, respectively,
311 while *ZmSKUs5* is approximately 4.2 Kb in length. Within the short arm of chromosome
312 5, *ZmHMA1* and *ZmSKUs5* are separated by 9.16 Mb, with *ZmHMA1* approximately 15
313 Mb away from the maximum likelihood prediction of a QTL involved in maize
314 domestication (Doebley and Stec 1993; Vielle-Calzada et al. 2009). *ZmHMA7* maps to the
315 centromeric region of chromosome 5. A detailed PlantCARE-based analysis identified
316 several conserved binding sites and regulatory elements in the promoter region of these
317 three genes (Lescot et al. 2002). *ZmHMA1* and *ZmHMA7* share binding sites to basic Helix-
318 Loop-Helix (bHLH) transcription factors, as well as abscisic acid response (ABRE),
319 ethylene responsive (ERF), and G-box (CACGTG) elements recognized by leucine zipper
320 family (bZIP) and bHLH transcription factors (Figure 3a). The regulatory region of both
321 *ZmHMA1* and *ZmSKUs5* contain a binding site for MIKC-type MADS box transcription
322 factors (Figure 3a), whereas *ZmHMA7* and *ZmSKUs5* share a jasmonic acid-response
323 TGACG-motif (Figure 3a), as well as a Myb-binding (MBS) and GATA binding site. In
324 addition, *ZmHMA1* contains a binding site for TCP proteins such as Tb1, increasing the
325 number of families of transcription factors that could be involved in shared or individual
326 regulation of these three genes (Figure 3a).
327
328 To elucidate the expression patterns of *ZmHMA1* and *ZmHMA7*, we conducted reverse
329 transcriptase PCR (RT-PCR) in leaves, stems, roots, and flowers at two vegetative (V2 and
330 V6) and one reproductive (R1) developmental stage, in teosinte *parviglumis* and wild-type
331 W22 maize individuals (Figure 3b). In the case of maize, *ZmHMA1* was expressed in
332 leaves, stems, roots and flowers throughout development in either absence or presence of

333 HMs. *ZmHMA7* was also expressed in aerial organs throughout development in both
334 absence and presence of HMs but was not expressed in roots at reproductive stage R1. In
335 teosinte *parviglumis, ZmHMA1* was also expressed throughout development in either
336 absence or presence of HMs. By contrast, ZmHMA*7* was constitutively expressed in aerial
337 organs, but only expressed in roots under HM stress during V2 and V6 stages. To further
338 determine if the level of expression of these two genes is influenced by the presence of
339 HMs, we conducted quantitative real-time PCR (qPCR) using the primary root of teosinte
340 *parviglumis* and maize plantlets at four weeks after germination (Figures 3c and 3d). In
341 wild-type W22 maize, the expression of *ZmHMA1* was not significantly different in the
342 presence and absence of HMs. By contrast, in teosinte *parviglumis* the expression of
343 *ZMHMA1* was significantly increased in presence of HMs (Figure 3c). In the case of
344 *ZmHMA7*, expression was significantly increased in both maize and teosinte *parviglumis*
345 when plants were grown in the presence of HMs (Figure 3d). Overall, these results indicate
346 that the activity of both *ZmHMA1* and *ZmHMA7* is influenced by HM stress in teosinte
347 *parviglumis* and maize.
348
349
350 ***ZmHMA1 null mutant individuals show phenotypic defects related to the domestication***
351 ***syndrome.***
352
353 Transposon *Mu* insertional lines have been widely used to elucidate gene function in maize.
354 To elucidate the function of *ZmHMA1*, we phenotypically analyzed *LANMu1029790*, a 4-
355 generation backcross of line *mu1029790* into the W22 background selected for single copy
356 insertions in *ZmHMA1* (McCarty et al. 2005). In *LANMu1029790,* a single *Mu* insertion is
357 in the first exon of *ZmHMA1*, 65 bp downstream of the START codon (Figure 3a). RT-
358 PCR analysis showed that expression of Z*mHMA1* is completely absent in homozygous
359 individuals for the *LANMu1029790* insertion (Figure S3), confirming that the

360 corresponding mutant is a null allele. Plants harboring a homozygous *LANMu1029790*
361 insertion are subsequently designated as *zmhma1-m1::MuDR* (abbreviated *zmhma1-m1*).
362
363 To determine the function of *ZmHMA1* in maize, we compared the phenotype of wild-type
364 W22 and homozygous *zmhma1-m1* individuals at the reproductive R1 stage (Table 2).
365 Under normal growing conditions, homozygous *zmhma1-m1* individuals generated
366 significantly less leaves than wild-type (NL = 13.4 ± 0.84 in wild-type, and NL = 11.4 ±
367 0.84 in *zmhma1-m1; P<0.001*). Whereas the length of mutant leaves was smaller than wild-
368 type (LML = 77.4 ± 6.64 cm in wild-type, and LML = 69.85 ± 9.18 cm in *zmhma1-m1*),
369 their width was significantly larger (WML = 6.75 ± 1.3 cm in wild-type, and WML = 9.75
370 ± 1.4 cm in *zmhma1-m1*; P<0.001), resulting in an increase of the total dry weight of aerial
371 organs in mutant plants (DWAP = 18.43 ± 8.04 grams in wild-type, and DWAP = 28.46 ±
372 9.54 grams in *zmhma1-m1*). Homozygous *zmhma1-m1* individuals also produced
373 significantly more female inflorescences per plant (NFI = 1.2 ± 0.42 in wild-type, and NFI
374 = 1.9 ± 0.32 in *zmhma1*; P<0.001) a difference that reflected in the total dry weight of
375 female inflorescences per plant (WFI = 40.06 ± 14.39 gr in wild-type and WFI = 69.5 ±
376 11.2 gr in *zmhma1*; P<0.001); and significantly more spikes per male inflorescence (NSB
377 = 9 ± 1.63 in wild-type, and NSB = 13.4 ± 2.32 in *zmhma1-m1*; P<0.001). Interestingly,
378 the general length of roots was significantly smaller in homozygous *zmhma1-m1*
379 individuals, in particular nodal roots (LNR = 87.2 ± 16.8 cm in wild-type, and LNR = 50.9
380 ± 12.83 cm in *zmhma1-m1*; P<0.001); however, mutant plants showed a significant
381 increase in the number of seminal roots per plant (NSR = 4.1 ± 1.45 in wild-type, and NSR
382 = 7.3 ± 1.16 in *zmhma1-m1*; P<0.001). When wild-type and mutant individuals were grown
383 under HM stress, differences in the size of leaves, number of female inflorescences per
384 plant, and number of spikes per male inflorescence were maintained. In addition, mutant
385 individuals exposed to HM stress were significantly taller than wild-type (HEI = 82.2 ±
386 34.94 cm in wild-type, and HEI = 125.9 ± 18.81 cm in *zmhma1-m1*; P<0.01). In addition,
387 total root and seminal root length were equivalent in wild-type and mutant individuals,
388 mainly because the length of wild-type roots was significantly reduced under HM stress;
389 however, the number of seminal roots was again significantly higher in mutant individuals
390 (NSR = 6.6 ± 1.35 in wild-type, and NSR = 8.2 ± 1.62 in *zmhma1-m1*; P<0.05). These

391 results indicate that in maize aerial organs, *ZmHMA1* is involved in promoting leaf growth,
392 restricting the number of female inflorescences per plant, and restricting the number of
393 spikes in male inflorescences. In underground organs, *ZmHMA1* is involved in promoting
394 root growth and restricting the number of seminal roots per individual. Under HM stress,
395 *ZmHMA1* shows an additional role in restricting plant height, a function that was not
396 identified under normal growing conditions. Overall, these results suggest that *ZmHMA1*
397 is involved in the control of some of the aerial and underground phenotypic traits that
398 distinguish maize from teosinte *parviglumis,* especially under HM stress conditions.
399
400
401 ***Under heavy metal stress, Tb1 is overexpressed in the apical meristem of teosinte***
402 ***parviglumis.***
403
404 The absence of secondary ramifications in teosinte *parviglumis* grown under HM stress is
405 reminiscent of the aerial architecture of wild-type maize. Previous QTL and molecular
406 analysis suggested that *Tb1* contributed to the architectural difference between maize and
407 teosinte, as *tb1* maize mutants develop secondary stem ramifications ending in male
408 inflorescences, resembling teosinte in their overall architecture (Doebley et al. 1997)
409 Interestingly, the regulatory region of *ZmHMA1* contains a specific binding site for
410 members of the Teosinte-branched 1/Cycloidea/Proliferating (TCP) family of transcription
411 factors that includes Tb1 (Figure 3a). To investigate the possibility that the phenotypic
412 response of teosinte *parviglumis* under HM stress could be regulated by *Tb1*, we conducted
413 quantitative real-time PCR (qPCR) to determine the expression of *ZmHMA1* and *Tb1* in
414 the shoot apical meristem (SAM) of one month old W22 maize and teosinte *parviglumis*
415 plantlets (Figure 4a and 4b). The expression *ZmHMA1* was downregulated in W22 wild-
416 type maize meristems in the presence of HMs. By contrast, HM stress resulted in a
417 significant increase of *ZmHMA1* expression in teosinte *parviglumis*, confirming that in the
418 maize ancestor the level of *ZmHMA1* activity is influenced by the presence of HMs in the
419 soil. In addition, the expression of *Tb1* was significantly upregulated in teosinte
420 *parviglumis* meristems in the presence of HMs, suggesting that formation of secondary
421 ramifications in teosinte *parviglumis* is repressed by *Tb1* function under HM stress. Taken

422 together, these results open the possibility for a direct positive regulation of *ZmHMA1* by
423 transcriptions factor of the TCP family, including *Tb1*.
424
425 **Discussion**
426
427 Although the evolutionary transition from teosinte *parviglumis* to maize resulted in
428 important phenotypic divergence between landraces and their wild progenitor, the
429 relevance of teosinte *parviglumis* phenotypic plasticity and its genetic consequences during
430 domestication remain poorly understood. Our study offers the first evidence showing that
431 a specific environmental factor (heavy metal stress) influenced specific gene function
432 (heavy metal response ATPases) and human selection during the *parviglumis* to maize
433 transition. The comparison of HM responses between both subspecies indicates that
434 teosinte *parviglumis* phenotypically responds to HM stress acquiring phenotypes
435 reminiscent of maize. Whereas low temperatures and CO_2 concentrations also caused a
436 significant decrease in lateral branching, these environmental response has not been related
437 to specific gene function and human selection. The absence of tillering exhibited by
438 teosinte *parviglumi*s under HM stress was not reported under conditions simulating an
439 early Holocene environment (Piperno et al., 2015). Our results also show an increase in the
440 number of female inflorescences per plant. This HM stress-dependent proliferation of
441 several closely associated female inflorescences in a single teosinte *parviglumis* stem has
442 not been previously reported. Female inflorescences arose from individual axillary
443 meristems in multiple internodes, significantly increasing teosinte *parviglumis* seed yield.
444 Our evidence indicates that HM stress revealed a teosinte *parviglumis* environmental
445 plasticity that is directly related to the function of specific HM response genes that were
446 affected by domestication through human selection.
447
448 We also show that *ZmHMA1*, *ZmHMA7* and *ZmSKUs5* exhibit reduced genetic diversity in
449 extant maize as compared to teosinte *parviglumis*, suggesting that all three loci were
450 affected by the evolutionary transition that gave rise to maize. The maize regulatory region
451 and downstream 3' area of the *ZmHMA1* locus exhibit pronounced reduction in SNPs
452 compared to teosinte *parviglumis* lines, likely affecting the molecular scope of its

453 regulatory proteins, including transcription factors of the TCP family (Martín-Trillo and
454 Cubas 2010). By contrast, *ZmHMA7* and *ZmSKUs5* showed a selective sweep across the
455 entire maize locus. Although loss of genetic diversity is usually the result of human
456 selection during domestication, it can also represent a consequence of natural selective
457 pressures favoring fitness of specific teosinte *parviglumis* allelic variants better adapted to
458 environmental changes and subsequently affected by human selection during the
459 domestication process. The significant reduction of nucleotide variability in the *ZmHMA1*
460 locus of teosinte *parviglumis* suggests that indeed that a natural selection pressure
461 Examples of edaphological factors driving genetic divergence in the teosintes or maize
462 include local adaptation to phosphorus concentration in *mexicana* and *parviglumis*
463 (Aguirre-Liguori et al. 2019), and fast maize adaptation to changing iron availability
464 through the action of genes involved in its mobilization, uptake, and transport (Benke and
465 Stich 2011).
466
467 The maize genome contains 12 genes encoding for members of the P1b family of ATPases
468 (Cao et al. 2019). They are subdivided according to their preferential substrate affinity: the
469 Copper (Cu)/Silver (Ag) group includes *ZmHMA1* to *ZmHMA4*; and the Zinc (Zn)/Cobalt
470 (Co)/Cadmium (Cd)/Lead (Pb) includes *ZmHMA5* to *ZmHMA12*. Initial studies suggested
471 that *ZmHMA1* is expressed at low levels in vegetative, reproductive or root organs
472 throughout development, contrary to *ZmHMA7* that is strongly expressed in developing
473 seeds 10 days after pollination; however, both genes appeared downregulated in plants
474 grown under either Cu or Cd stress (Zhiguo et al. 2018). Additional studies by Cao et al
475 (2019) indicated low expression of *ZmHMA1* and high levels of *ZmHMA7* expression in
476 12 tissues: roots, nodes, shoots, leaves, tassel, shoot apical meristem and young stem,
477 internodes, anthers, silks, whole seedlings, endosperm, embryo, and pericarp. Under Cd
478 stress, expression of both *ZmHMA1* and *ZmHMA7* was significantly upregulated in roots
479 and downregulated in stems (Cao et al. 2019), contradicting previous results by Zhiguo et
480 al. (2018). In Arabidopsis and barley, the corresponding *ZmHMA1* structural homologs
481 (*AtHMA1* and *HvHMA1*, respectively) can transport a wide range of metals into the
482 chloroplast (Mikkelsen et al. 2012; Boutigny et al. 2014). In the case of the Arabidopsis
483 structural homolog of ZmHMA7, AtHMA7 (also called RAN1) is proposed to act as a

484 metallochaperone located in the Golgi apparatus, delivering Cu to the ethylene receptor
485 located in the plasma membrane (Hirayama et al. 1999). Our evidence complements
486 previous studies by showing that, in maize, *ZmHMA1* root expression is restricted to
487 vegetative developmental stages, and that *ZmHMA7* is expressed in roots in response to
488 HM stress. We also show through qPCR analysis that, under HM stress, the expression of
489 both *ZmHMA1* and *ZmHMA7* is upregulated in teosinte *parviglumis* primary roots of 4-
490 week-old plantlets. Overall, these results confirm that both *ZmHMA1* and *ZmHMA7* are
491 heavy metal response genes active throughout teosinte and maize development.
492
493 In maize, the phenotypic analysis of null mutant individuals indicates that *ZmHMA1* is
494 involved in the control of aerial and underground developmental traits, some of which are
495 related to important functional adaptations that distinguish maize from its wild ancestor. In
496 addition to changes in leaf number, leaf length, and number of spikes per male
497 inflorescence, *zmhma1-m1* mutant individuals grown under normal edaphological
498 conditions showed a significant increase in the number of female inflorescences per plant,
499 a significant reduction in the length of nodal roots, and a significant increase in the number
500 of seminal roots per plant. Whereas the promotion of nodal root growth is a distinctive trait
501 of maize phenotypic plasticity and adaptation, previous studies showed that contrary to
502 maize, plants of teosinte *parviglumis* lack seminal roots. This absence is also characteristic
503 of paleobotanical maize specimens dating more than 5,000 years before present,
504 confirming that the acquisition of seminal roots is an important trait acquired during
505 domestication (Lopez-Valdivia et al. 2022). The presence of seminal roots distinguishes
506 extant maize from the teosintes (Burton et al. 2013), suggesting a possible involvement in
507 domestication (Perkins and Lynch 2021; Lopez-Valdivia et al. 2022). Our results suggest
508 that the allelic variants of the *ZmHMA1* locus selected during domestication could have
509 contributed to promote seminal root formation in maize, optimizing their number in
510 accordance to seed endosperm availability and carbohydrate reserves (Perkins and Lynch
511 2021; Lopez-Valdivia et al. 2022). Interestingly, *ZmHMA1* plays an important role in
512 contributing to restricting plant height in response to HM stress, a phenotype that is also
513 an important distinction between teosinte *parviglumis* and maize. Taken together, these
514 results indicate that *ZmHMA1* function was involved in the phenotypic transition from

515 teosinte *parviglumis* to maize through the influence of HM stress; however, a better
516 definition of its role in the origin and domestication of maize will require a functional
517 analysis of the *ZmHMA1* teosinte *parviglumis* homolog, and a detailed molecular analysis
518 of the corresponding allelic variants and their phenotypic effects in both subspecies.
519
520 ***Ideas and Speculation.***
521
522 Our results point to an evolutionary model in which environmental changes in the form of
523 edaphological HM stress imposed natural selective forces that acted on native teosinte
524 *parviglumis* populations, causing phenotypic responses and a severe genetic bottleneck
525 (Figure S4). Adapted plants developed phenotypic traits such as shorter height and
526 emergence of seminal roots, progressively giving raise to primitive maize individuals with
527 reduced genetic variation in HM response genes such as *ZmHMA1*. The subsequent action
528 of human selection caused a drastic reduction in allelic variation of heavy metal response
529 genes, and genetic fixation of the resulting domestication traits.
530
531 The most important source of HMs in ancient soils of Mesoamerica is volcanic activity
532 through short- and long-term effects related to ores, hydrothermal water flow and ash
533 deposits. The history of eruptive activity in the Trans Mexican Volcanic Belt during the
534 early Holocene coincides with the temporal estimation of initial stages in the evolutionary
535 transition that gave rise to maize. Intense and recurrent eruptions occurred 24,000 to 6,000
536 years ago near the region of the Balsas River basin presumed to be the cradle of maize
537 domestication (Matsuoka et al. 2002; Macias 2005). Located less than 100 Km from the
538 region that harbors the natural teosinte *parviglumis* populations most closely related to
539 maize (Matsuoka et al. 2002), the Nevado de Toluca volcano underwent four major
540 eruptions approximately 24100, 12100, 10500, and 8500 years before present (yr BP;
541 Macias 2005), causing in the region a period of climatic instability that lasted until 8500
542 yr BP (Ludlow-Wiechers et al., 2005). Could volcanic eruptions during the early Holocene
543 have modified soil composition and influence the initial evolutionary transition from
544 teosinte *parviglumis* to primitive maize? The possibility of environmental cues influencing
545 maize emergence was mentioned by Benz and Iltis (1992), but not in relation to volcanic

546 activity. Deciphering the ancient DNA sequence of HM response genes such as *ZmHMA1*
547 in paleobotanical maize specimens found in Central Mexico could help determine if its
548 genetic diversity was already reduced by 5,300 to 6,200 yr BP (Ramos-Madrigal et al.,
549 2016 ; Vallebueno-Estrada et al., 2016; Benz, 2001). Our results open the possibility for
550 environmental changes caused by volcanic activity acting as a driving force in the selection
551 of loci involved in adaptive responses such as heavy metal tolerance.
552
553
554 **Materials and Methods**
555
556 *Plant materials and growth conditions.*
557 Seeds from maize inbred line W22, teosinte *parviglumis* accession CIMMYTMA 29791,
558 and insertional line *LANMu1029790* were sterilized using a 1:1 distilled water and bleach
559 solution, rinsed three times in water, and germinated in MS solid medium. One week-old
560 seedings were transplanted into PVC tubes (length: 90 cm; diameter: 20 cm) or 20-liter
561 pots filled with a pre-sterilized mix composed of 30% peat moss, 10% vermiculite, 10%
562 perlite, and 50% ground litter, complemented with 15-9-12 (N-P-K) Osmocote^{TM} fertilizer.
563 For HM growth conditions, 16 mg/kg of cadmium chloride ($CdCl_2$) and 400 mg/kg of
564 copper sulfate ($CuSO_4$) were added to the substrate before seedling transplant. All plants
565 were grown under glasshouse conditions at 28°C during day and 24°C during night, with
566 relative humidity comprised between 40 and 50%.
567
568 *Phenotypic analysis.*
569 All plants were harvested at 15 days (V2 stage), 30 days (V6 stage), and 50 days (R1 stage)
570 after transplant. No less than ten plants were measured for each trait and stage. The width
571 and length of immature leaves was measured in the 5th leaf. The length and width of mature
572 leaves in the 3rd leaf. The total number of leaves, total number of stem internodes, plant
573 height, basal stem diameter, total number of stem ramifications, and total fresh and dry
574 weight of the aerial biomass were estimated at the R1 stage. Estimated root traits included
575 the number and length of brace roots (aerial roots), the number and length of crown roots
576 (underground roots originating within 2 cm below the basal node), number and length of

577 nodal roots (underground roots originating more than 2 cm below the basal node), the
578 number and length of seminal roots and maximum length of the root system.
579
580
581 *Genetic diversity analysis.*
582 The SNP collection of maize chromosome 5 was analyzed on the basis of the HapMap
583 V3.2.1 dataset (Bukowski et al. 2018), selecting individuals from maize landraces (LR)
584 (Table S6) and teosinte *parviglumis* inbred line accessions (Teo; Table S7). A sliding
585 window diversity (π) was calculated using VCFtools v0.1.13 (Danecek et al. 2011) with a
586 window size of 100 bp (--window-pi 100) and a sliding step of 50 bp (--window-pi-step
587 50). Regions under selection were extracted from a list of 304 genes with domestication-
588 related selection signatures across the whole chromosome (Hufford et al. 2012; Tables S8),
589 for a total of 385,829 sliding windows (Table S9 and S10). A second set of neutral gene
590 regions comprising 2,373,010 windows was also extracted across the entirety of
591 chromosome 5. These two collections were compared to *ZmHMA1* (GRMZM2G067853),
592 *ZmHMA7* (GRMZM2G029951), and *ZmSKUs5* (GRMZM2G076985), encompassing
593 2,743 windows (Table S11 and S12). Additionally, we analyzed genetic diversity in the
594 neighboring regions of these candidate genes, which included six genes
595 (*GRMZM2G701784*, *GRMZM2G014508*, *GRMZM2G367857*, *GRMZM2G375607*,
596 *GRMZM2G374375*, and *GRMZM2G067883*), totaling 3,088 windows. We employed a
597 custom Perl script (Vallebueno GitHub repository) to calculate two diversity metrics: fold
598 change (FC= π(LR)/π(Teo)) and the proportional diversity (FP=π(LR)/(π(LR) + π(Teo)).
599 Data visualization was performed using violin plots generated in R v4.2.2.
600
601 For an arbitrary locus encompassing 30 Kbs up and downstream of the coding sequence of
602 *ZmMA1*, *ZmHMA7*, and *ZmSKUs5*, the number of segregating sites (S), the number of
603 unique sequences (haplotypes, h), and the nucleotide diversity index (θ) were estimated
604 using DnaSP version 6.0 for all accessions included in HapMap3 (Rozas et al. 2017;
605 Bukowski et al. 2018). DnaSP was also used to estimate Tajima's D, Fu and Li's D, and
606 Fu and Li's F indexes (Tajima 1989; Fu and Li 1993). The average proportion of pairwise
607 nucleotide differences per nucleotide site (π) was calculated with VCFtools using bins of

608 100 bp and steps of 25 bp (Tajima 1983; Weir and Cockerham 1984). Null hypothesis of
609 equality of parameters followed two-tailed tests as previously described (Rozas et al.
610 2017).
611
612
613 *Gene expression analysis.*
614 Leaves, stems, tassels, female inflorescences, as well as primary, nodal, and crown roots
615 were manually isolated, frozen in liquid nitrogen and stored at 4°C. Total RNA was
616 extracted using TRIZOL (Thermo Fisher Scientific, USA). For reverse-transcriptase PCR
617 (RT-PCR), RNA was converted to coding DNA using the One-step RT-PCR kit (QIAGEN,
618 USA). The full list of primers is presented in Table S8. *ZmCDK* was used as a positive
619 control. PCR amplification was conducted using the following parameters: at 94°C for 5
620 min.; 94°C 30 sec., 60°C 30 sec., 72°C 1 min. for 35 cycles; final stop after 72°C for 10
621 min. For quantitative real-time PCR (qPCR), total RNA was isolated from 4-week-old
622 meristems using TRIZOL. Complementary DNA (cDNA) was synthesized using 4 µg of
623 total RNA, 10 mM oligodTs and Superscript reverse transcriptase II (Invitrogen, USA).
624 Primers for PCR were designed using the online program Primer 3 Plus (v.0.4.0) and
625 verified with Oligocalculator (Sigma Chemical, St Louis MO) to discard dimer formation.
626 PCR efficiencies of target and reference gene were determined by generating standard
627 curves based on serial dilutions prepared for cDNA templates. PCR efficiency was
628 calculated according to the slope of the standard curve (primers with 100% efficiency, the
629 fold equals 2). Each quantitative real-time PCR (qPCR) reaction was performed in a 10 µl
630 volume consisting of 5 µl of 23 SYBR Green PCR reaction Mix (Applied Biosystems,
631 Foster City, CA). 3.5 µl of the DNA template (100 ng/ml), 0.5 µl of the forward primer (5
632 mM), 0.5 µl of the reverse primer (5 mM), and 0.5 µl of ultrapure water. The qPCR
633 reactions were performed using the CFX96 Touch Real-Time PCR detection System and
634 the data were analyzed using the Bio-Rad CFX Manager software v3.1. The thermal profile
635 consisted of 10 min at 95°C, 40 cycles of 15 sec at 95°C, and 1 min at 60°C. Amplification
636 results were collected at the end of the extension step. Primer sequences for qPCR
637 amplification are listed in Table S7. A comparative 2-ΔΔCT method was used for
638 determining a relative target quantity of gene expression (Schefe et al. 2006), and the

639 cyclin-dependent kinase gene *ZmCDK* (GRMZM2G149286) was used as a control (Hu et
640 al. 2019). Reproducibility of the results was evaluated for each sample by running three
641 technical and three biological replicates of each of the reactions and each sample.
642
643 *Statistical Analysis.*
644 Statistical analyses were conducted using RStudio, version 4.3.0 (Horton and Kleinman
645 2015). The data are presented as mean ± standard deviation and were tested by a paired
646 Student's T-Test. When the effects were significant according to T-Test, the treatments
647 were compared with the Welch two sample T-Test at $P < 0.05$.
648

649 **Acknowledgments**

650 We would like to thank Ueli Grossniklaus for critical comments of this manuscript; Juana
651 de la Cruz for supporting greenhouse activities; Ivan López-Valdivia, Eduardo González-
652 Orozco and Cristian Eduardo Martínez Guerrero for help with bioinformatic analysis; and
653 Enrique Pola for help with qPCR analysis. All members of the Apolab offered valuable
654 suggestions and support. This research was funded by Conahcyt grant (CB-256826) and
655 the INAH-Cinvestav Tehuacán Collaborative Initiative. J.A.-B. is the recipient of a
656 graduate scholarship from Consejo Nacional de Humanidades Ciencia y Tecnologia
657 (CONAHCyT).
658

659 **Competing interests**

660 None declared.
661

662 **Author contributions**

663 J. A-B and J.P. V-C designed the study. J. A-B and J.P. V-C coordinated and managed the
664 project. M.V.E. designed and performed computational analysis. J. gfrtcdA-B performed
665 the experiments, J. A-B, M.V.E and J.P. V-C analyzed and interpreted the data, J. A-B and
666 J.P. V-C wrote the article. All authors read and approved the final version of the
667 manuscript.
668

List of References

AbdElgawad H, Zinta G, Hamed BA, Selim S, Beemster G, Hozzein WN, Wadaan MAM, Asard H, Abuelsoud W. 2020. Maize roots and shoots show distinct profiles of oxidative stress and antioxidant defense under heavy metal toxicity. *Environmental Pollution* 258: 113705.

Acosta-Bayona J, León-Martínez G, Vielle-Calzada JP. 2024. Origin and diversification of maize: two teosintes but different contributions. *Molecular Plant* 17: 233–235.

Aguirre-Liguori JA, Gaut BS, Jaramillo-Correa JP, Tenaillon MI, Montes-Hernández S, García- Oliva F, Hearne SJ, Eguiarte LE. 2019. Divergence with gene flow is driven by local adaptation to temperature and soil phosphorus concentration in teosinte subspecies (*Zea mays parviglumi*s and *Zea mays mexicana*). *Molecular Ecology* 28: 2814–2830.

Atta MI, Zehra SS, Ali H, Ali B, Abbas SN, Aimen S, Sarwar S, Ahmad I, Hussain M, Al-Ashkar I, Elango D, Sabagh AE, et al. 2023. Assessing the effect of heavy metals on maize (*Zea mays L*.) growth and soil characteristics: Plants-implications for phytoremediation. *PeerJ* 11: e16067.

Axelsen KB, Palmgren MG. 2001. Inventory of the superfamily of P-Type ion pumps in *Arabidopsis*. *Plant Physiology* 126: 696-706.

Benke A, Stich B. 2011. An analysis of selection on candidate genes for regulation, mobilization, uptake, and transport of iron in maize. *Genome* 54: 674–683.

Benz B. 2001. Archaelogical evidence of teosinte domestication from Guilá Naquitz, Oaxaca. *Proceedings of the National Academy of Sciences USA* 98:2104-2106.

Bomblies K, Doebley JF. 2006. Pleiotropic effects of the duplicate maize *FLORICAULA/LEAFY* genes *zfl1* and *zfl2* on traits under selection during maize domestication. *Genetics* 172: 519–531.

Boutigny S, Sautron E, Finazzi G, Rivasseau C, Frelet-Barrand A, Pilon M, Rolland N, Seigneurin-Berny D. 2014. HMA1 and PAA1, two chloroplast-envelope PIB-ATPases, play distinct roles in chloroplast copper homeostasis. *Journal of Experimental Botany* 65: 1529–1540.

Bukowski R, Guo X, Lu Y, Zou C, He B, Rong Z, Wang B, Xu D, Yang B, Xie C, Fan L, Gao S, Xu X, Zhang G, Li Y, Jiao Y, Doebley JF, Ross-Ibarra J, Lorant A, Buffalo V, Cinta Romay M, Buckler ES, Ware D, Lai J, Sun Q, Xu Y. 2018. Construction of the third-generation *Zea mays* haplotype map. *GigaScience* 7: 1-12.

Burton AL, Brown KM, Lynch JP. 2013. Phenotypic diversity of root anatomical and architectural traits in *Zea* species. *Crop Science* 53: 1042–1055.

Cao Y, Zhao X, Liu Y, Wang Y, Wu W, Jiang Y, Liao C, Xu X, Gao S, Shen Y, Lan H, Zou C, Pan G, Lin H, et al. 2019. Genome-wide identification of *ZmHMAs* and association of natural variation in *ZmHMA2* and *ZmHMA3* with leaf cadmium accumulation in maize. *PeerJ* 7: e7877.

Chen Z, Sun J, Li D, Li P, He K, Ali F, Mi G, Chen F, Yuan L, Pan Q, et al. 2022. Plasticity of root anatomy during domestication of a maize-teosinte derived population. *Journal of Experimental Botany* 73: 139–153.

Danecek, Petr, Adam Auton, Goncalo Abecasis, Cornelis A. Albers, Eric Banks, Mark A. DePristo, Robert E. Handsaker, et al. 2011. The Variant Call Format and VCFtools. *Bioinformatics* 27(15): 2156–2158.

731 **Doebley J, Stec A. 1993.** Inheritance of the morphological differences between maize and
732 teosinte: comparison of results for two F2 populations. *Genetics* 134: 559-570.
733
734 **Doebley J, Stec A, Hubbard L. 1997.** The evolution of apical dominance in maize. *Nature*
735 6724: 236-239.
736
737 **Eyre-Walker A, Gaut RL, Hilton H, Feldman DL, Gaut BS. 1998.** Investigation of the
738 bottleneck leading to the domestication of maize. *PNAS* 95: 4441-4446.
739
740 **Fu Y-X, Li W-H. 1993.** Statistical tests of neutrality of mutations. *Genetics* 133: 693-709.
741
742 **Gallo-Franco JJ, Sosa CC, Ghneim-Herrera T, Quimbaya M. 2020.** Epigenetic control
743 of plant response to heavy metal stress: a new view on aluminum tolerance. *Frontiers*
744 *in Plant Science* 11: 602625.
745
746 **Gao C, Gao K, Yang H, Ju T, Zhu J, Tang Z, Zhao L, Chen Q. 2022.** Genome-wide
747 analysis of metallothionein gene family in maize to reveal its role in development and
748 stress resistance to heavy metal. *Biological Research* 55:1.
749
750 **Gaudin ACM, McClymont SA, Raizada MN. 2011.** The nitrogen adaptation strategy of
751 the wild teosinte ancestor of modern maize, *Zea mays* subsp. *parviglumis*. *Crop*
752 *Science* 51: 2780–2795.
753
754 **Hall JL. 2002.** Cellular mechanisms of heavy metal detoxification and tolerance. *Journal*
755 *of Experimental Botany* 53: 1-11.
756
757 **Hirayama T, Kieber JJ, Hirayama N, Kogan M, Guzman P, Nourizadeh S, Alonso**
758 **JM, Dailey WP, Dancis A, Ecker JR, et al. 1999.** RESPONSIVE-TO-
759 ANTAGONIST1, a Menkes/Wilson disease-related copper transporter, is required for
760 ethylene signaling in *Arabidopsis*. *Cell* 97: 383-393.
761

Horton NJ, Kleinman, K. 2015. Using R and RStudio for data management, statistical analysis, and graphics second edition. New York, US: Chapman and Hall/CRC.

Hu B, Jiang Z, Wang W, Qiu Y, Zhang Z, Liu Y, Li A, Gao X, Liu L, Qian Y, Huang X, Yu F, Kang S, Wang Y, Xie J, Cao S, Zhang L, Wang Y, Xie Q, Kopriva S, Chu C, et al. 2019. Nitrate–NRT1.1B–SPX4 cascade integrates nitrogen and phosphorus signaling networks in plants. *Nature Plants* 5: 401–413.

Hufford, Matthew B., Xun Xu, Joost van Heerwaarden, Tanja Pyhäjärvi, Jer-Ming Chia, Reed A. Cartwright, Robert J. Elshire, et al. 2012. Comparative population genomics of maize domestication and mprovement. *Nature Genetics* 44 (7): 808–11.

Benz BF, Iltis HH. 1992. Evolution of Female Sexuality in the Maize Ear (Zea Mays L. subsp. Mays-Gramineae). *Economic Botany* 46: 212–22.

Larson G, Piperno DR, Allaby RG, Purugganan MD, Andersson L, Arroyo-Kalin M, Barton L, Vigueira CC, Denham T, Dobney K, Doust AN, Gepts P, Thomas M Gilbert P, Gremillion KJ, Lucas L, Lukens L, Marshall FB, Olsen KM, Pires JC, Richerson PJ, Rubio De Casas R, Sanjur OI, Thomas MG, Fuller DQ, et al. 2014. Current perspectives and the future of domestication studies. *PNAS* 111: 6139–6146.

Lescot M, Déhais P, Thijs G, Marchal K, Moreau Y, Van de Peer Y, Rouzé P, Rombauts S. 2002. PlantCARE, a database of plant *cis*-acting regulatory elements and a portal to tools for *in silico* analysis of promoter sequences. *Nucleic Acids Research* 30: 325–327.

Lopez-Valdivia I, Perkins AC, Schneider HM, Vallebueno-Estrada M, Burridge JD, Gonzalez-Orozco E, Montufar A, Montiel R, Lynch JP, Vielle-Calzada JP, et al. 2022. Gradual domestication of root traits in the earliest maize from Tehuacán. *PNAS* 119: e2110245119.

Lorant A, Ross-Ibarra J, Tenaillon M. 2020. Genomics of long- and short-term adaptation in maize and teosintes. *Methods in Molecular Biology* 2090: 289-311.

Ludlow-Wiechers B, Almeida-Leñero L, Isble G. 2005. Paleoecological and climatic changes of the Upper Lerma Basin, Central Mexico during the Holocene. *Quaternary Research* 64: 318-332.

Macías JL. 2005. Geología e historia eruptiva de algunos de los grandes volcanes activos de México. *Boletín De La Sociedad Geológica Mexicana*. 107: 379-424.

Malenica N, Dunić JA, Vukadinović L, Cesar V, Šimić D. 2021. Genetic approaches to enhance multiple stress tolerance in maize. *Genes* 12:1760.

Martín-Trillo M, Cubas P. 2010. TCP genes: a family snapshot ten years later. *Trends in Plant Science* 15: 31–39.

Matsuoka Y, Vigouroux Y, Goodman MM, Sanchez JG, Buckler E, Doebley J. 2002. A single domestication for maize shown by multilocus microsatellite genotyping. *PNAS* 99: 6080-6084.

McCarty DR, Mark Settles A, Suzuki M, Tan BC, Latshaw S, Porch T, Robin K, Baier J, Avigne W, Lai J, Messing J, Koch KE, Curtis Hannah L, et al. 2005. Steady-state transposon mutagenesis in inbred maize. *Plant Journal* 44: 52–61.

Mikkelsen MD, Pedas P, Schiller M, Vincze E, Mills RF, Borg S, Møller A, Schjoerring JK, Williams LE, Baekgaard L, Holm PB, Palmgren MG, et al. 2012. Barley *HvHMA1* is a heavy metal pump involved in mobilizing organellar Zn and Cu and plays a role in metal loading into grains. *PLoS ONE* 7: e49027.

823 **Perkins AC, Lynch JP. 2021.** Increased seminal root number associated with
824 domestication improves nitrogen and phosphorus acquisition in maize seedlings.
825 *Annals of Botany* 128: 453–468.
826
827 **Pickersgill B. 2007.** Domestication of plants in the Americas: insights from mendelian and
828 molecular genetics. *Annals of Botany* 100: 925–940.
829
830 **Piperno DR, Holst I, Winter K, McMillan O. 2015.** Teosinte before domestication:
831 experimental study of growth and phenotypic variability in late Pleistocene and early
832 Holocene environments. *Quaternary International* 363: 65–77.
833
834 **Ramos-Madrigal J, Smith BD, Moreno-Mayar J, Gopalakrishnan S, Ross-Ibarra J,**
835 **Gilbert MTP, Wales N. 2016.** Genome sequence of a 5,310-year-old maize cob
836 provides insights into the early stages of maize domestication. *Current Biology*
837 26:3195-3201
838
839 **Ren W, Zhao L, Liang J, Wang L, Chen L, Li P, Liu Z, Li X, Zhang Z, Li J, He K,**
840 **Zhao Z, Ali F, Mi G, Yan J, Zhang F, Chen F, Yuan L, Pan Q, et al. 2022.** Genome-
841 wide dissection of changes in maize root system architecture during modern breeding.
842 *Nature Plants* 8: 1408–1422.
843
844 **Ross-Ibarra J, Morrell PL, Gaut BS. 2007.** Plant domestication, a unique opportunity to
845 identify the genetic basis of adaptation. *PNAS* 104: 8641-8648.
846
847 **Rozas J, Ferrer-Mata A, Sanchez-Del Barrio JC, Guirao-Rico S, Librado P, Ramos-**
848 **Onsins SE, Sanchez-Gracia A. 2017.** DnaSP 6: DNA sequence polymorphism
849 analysis of large data sets. *Molecular Biology and Evolution* 34: 3299–3302.
850
851 **Schefe JH, Lehmann KE, Buschmann IR, Unger T, Funke-Kaiser H. 2006.**
852 Quantitative real-time RT-PCR data analysis: current concepts and the novel "gene
853 expression's CT difference" formula. *Journal of Molecular Medicine* 84: 901–910.

854

855 **Sedbrook JC, Carroll KL, Hung KF, Masson PH, Somerville CR. 2002.** The
856 *Arabidopsis SKU5* gene encodes an extracellular glycosyl phosphatidylinositol-
857 anchored glycoprotein involved in directional root growth. *Plant Cell* 14: 1635–1648.
858

859 **Sigmon B, Vollbrecht E. 2010.** Evidence of selection at the *ramosa1* locus during maize
860 domestication. *Molecular Ecology* 19: 1296–1311.
861

862 **Smeets K, Opdenakker K, Remans T, Van Sanden S, Van Belleghem F, Semane B,**
863 **Horemans N, Guisez Y, Vangronsveld J, Cuypers A, et al. 2009.** Oxidative stress-
864 related responses at transcriptional and enzymatic levels after exposure to Cd or Cu in
865 a multipollution context. *Journal of Plant Physiology* 166: 1982–1992.
866

867 **Solioz M, Vulpe C. 1996.** CPx-type ATPases: a class of P-type ATPases that pump heavy
868 metals. *Trends in Biochemical Sciences* 21: 237-241.
869

870 **Studer AJ, Wang H, Doebley JF. 2017.** Selection during maize domestication targeted a
871 gene network controlling plant and inflorescence architecture. *Genetics* 207: 755–765.
872

873 **Tajima F. 1983.** Evolutionary relationship of DNA sequences in finite populations.
874 *Genetics* 105: 437-460.
875

876 **Tajima F. 1989.** Statistical method for testing the neutral mutation hypothesis by DNA
877 polymorphism. *Genetics* 123: 585-595.
878

879 **Vallebueno-Estrada M, Rodriguez-Arevalo I, Rougon-Cardoso A, Martinez**
880 **Gonzalez J, Garcia Cook A, Montiel R, Vielle-Calzada JP. 2016.** The earliest
881 maize from San Marcos Tehuacán is a aprtial domesticate with genomic evidence of
882 inbreeding. *Proceedings of the National Academy of Sciences USA* 113:14151-14156.
883

884 **Vallebueno-Estrada M, Hernández-Robles G, González-Orozco E, López-Valdivia I,**
885 **Rosales-Tham T, Vásquez-Sánchez V, Swarts K, Dillehay T, Vielle-Calzada JP,**
886 **Montiel R, et al. 2023**. Domestication and lowland adaptation of coastal preceramic
887 maize from Paredones, Peru. *Elife* 12: e83149.
888
889 **Vielle-Calzada JP, De La Vega OM, Hernández-Guzmán G, Ibarra-LacLette E,**
890 **Alvarez-Mejía C, Vega-Arreguín JC, Jiménez-Moraila B, Fernández-Cortés A,**
891 **Corona-Armenta G, Herrera-Estrella L, Herrera-Estrella A. 2009.** The Palomero
892 genome suggests metal effects on domestication. *Science* 326: 1078.
893
894 **Voskoboinik I, Fernando R, Veldhuis N, Hannan KM, Marmy-Conus N, Pearson RB,**
895 **Camakaris J. 2003.** Protein kinase-dependent phosphorylation of the Menkes copper
896 P-type ATPase. *Biochemical and Biophysical Research Communications* 303: 337–
897 342.
898
899 **Wang H, Studer AJ, Zhao Q, Meeley R, Doebley JF. 2015.** Evidence that the origin of
900 naked kernels during maize domestication was caused by a single amino acid
901 substitution in *tga1*. *Genetics* 200: 965–974.
902
903 **Weir BS, Cockerham CC. 1984.** Estimating F-Statistics for the analysis of population
904 structure. *Evolution* 38: 1358-1370.
905
906 **Williams LE, Mills RF. 2005.** P1B-ATPases - an ancient family of transition metal pumps
907 with diverse functions in plants. *Trends in Plant Science* 10: 491–502.
908
909 **Wills DM, Whipple CJ, Takuno S, Kursel LE, Shannon LM, Ross-Ibarra J, Doebley**
910 **JF. 2013.** From many, one: genetic control of prolificacy during maize domestication.
911 *PLoS Genetics* 9: e1003604.
912
913 **Yang N, Wang Y, Liu X, Jin M, Vallebueno-Estrada M, Calfee E, Chen L, Dilkes BP,**
914 **Gui S, Fan X, Harper TK, Kennett DJ, Li W, Lu Y, Ding J, Chen Z, Luo J,**

Mambakkam S, Menon M, Snodgrass S, Veller C, Wu S, Wu S, Zhuo L, Xiao Y, Yang X, Stitzer MC, Runcie D, Yan J, Ross-Ibarra J, et al. 2023. Two teosintes made modern maize. *Science* 382: 1013–1021.

Zhiguo E, Tingting L, Chen C, Lei W. 2018. Genome-wide survey and expression analysis of P1B-ATPases in rice, maize and sorghum. *Rice Science* 25: 208–217.

Legend of Figures.

Figure 1. Phenotypic response of teosinte *parviglumis* and wild-type W22 maize grown under heavy metal stress. (**a**) to (**e**), teosinte *parviglumis*; (**f**) to (**j**), W22 maize. (**a**) Teosinte *parviglumis* in absence of heavy metal stress at early flowering stage. (**b**) Teosinte *parviglumis* grown under heavy metal stress at early flowering stage. (**c**) Teosinte *parviglumis* in absence of heavy metal stress at late flowering stage. (**d**) Teosinte *parviglumis* grown under heavy metal stress at late flowering stage. (**e**) Teosinte *parviglumis* showing proliferation of female inflorescences arising from independent axillary meristems under heavy metal stress (detail of d). (**f**) W22 maize in absence of heavy metal stress at early flowering stage. (**g**) W22 maize grown under heavy metal stress at early flowering stage. (**h**) W22 maize in absence of heavy metal stress at late flowering stage. (**i**) W22 maize grown under heavy metal stress at late flowering stage. (**j**) W22 maize female inflorescences at late flowering stage (detail of i). Scale bars: 10 cm.

Figure 2. Genetic diversity of loci encompassing *ZmHMA1, ZmHMA7*, and *ZmSKUs5.* The nucleotide variability index (π) was calculated for all HapMap3 accessions of teosinte *parviglumis* (blue line), maize (red line), and *Tripsacum dactyloides* (orange line), taking in consideration the coding sequence (arrow) and an upstream and downstream region of 15 Kb encompassing each gene. (**a**) Nucleotide variability in the *ZmHMA1* locus. (**b**) Nucleotide variability in the ZmHMA7 locus. (**c**) Nucleotide variability in the *ZmSKUs5* locus. (**d**) Nucleotide variability in the *ZmGLB1* locus.

Figure 3. Structure and gene expression of *ZmHMA1* and *ZmHMA7* in teosinte *parviglumis* and W22 maize. (**a**) Structural analysis of *ZmHMA1*, *ZmHMA7*, and *ZMSKUs5*. Blue triangles indicate the location of motifs predicted in the regulatory region of each gene. The insertion site of *Mu* line *LANMu1029790* is indicated by a red triangle. (**b**) RT-PCR analysis of *ZmHMA1* and *ZMHMA7* expression throughout development of teosinte *parviglumis* and W22 maize in presence or absence of heavy metal stress; L=leaf; S=stem; PR=primary root; NR=nodal root; CR=crown root. V2: 15 days after transplant; V6: 30 days after transplant; R1: 50 days after transplant. Controls: (-) absence of DNA;

(+) genomic DNA. (**c**) qPCR analysis of *ZmHMA1* expression in 1-month old primary roots, in absence or presence of heavy metal stress. (**d**) qPCR analysis of *ZmHMA7* expression in 1-month old primary roots, in absence or presence of heavy metal stress. * P<0.01; ** P<0.001.

Figure 4. *Tb1* and *ZmHMA1* expression in the shoot apical meristem of plantlets grown under heavy metal stress. (a) qPCR analysis of *Tb1* expression in 1-month old teosinte *parviglumis* plantlets grown in absence or presence of heavy metal stress. (**b**) qPCR analysis of *ZmHMA1* expression in 1-month old teosinte *parviglumis* and W22 maize plantlets in absence or presence of heavy metal stress. * P<0.01.

Legend of Appendix and Supplementary Files.

Figure S1. Cumulative plot of QTL detected in a region of chromosome five that includes *ZmSKUs5* and *ZmHMA1* (modified from Lemmon and Doebley, 2024).

Figure S2. Comparison of chromosome 5 nucleotide variability between maize landraces and teosinte *parviglumis*.

Figure S3. Expression of *ZmHMA1* in wild-type and homozygous *zmhma1* maize individuals.

Figure S4. Speculative model illustrating the influence of heavy metal stress on the evolutionary transition of teosinte *parviglumis* to maize.

Table S1. Additional estimation of phenotypic traits in teosinte *parviglumis* grown in absence or presence of heavy metal stress.

Table S2. Additional estimation of phenotypic traits in wild-type and *zmhma1* maize grown in absence or presence of heavy metal stress.

Table S3. Full comparison of phenotypic values for wild-type W22, *zmhma1*, and teosinte *parviglumis* individuals grown under absence or presence of heavy metal stress

Table S4. Nucleotide variability across the *ZmSKUS5, ZmHMA*1 and *ZmHMA7* locus; and their upstream and downstream neighboring genes in maize landraces, maize improved lines, and teosinte *parviglumi*s accessions included in HapMap3.

Table S5. Collection of primers used in this study.

Table S6. Maize landrace accessions used in the genetic diversity analysis chr5.

Table S7. Teosinte *parviglumis* accessions used in the genetic diversity analysis chr5.

Supplementary File 1. List of domestication genes present on chr5 as defined by Hufford et al. 2012

Supplementary File 2. FC and FP values for all domestication genes present in chr5.

Supplementary File 3. FC and FP values of neutral regions included in chr5.

Supplementary File 4. FC and FP values of candidate genes *ZmHMA1*, *ZmHMA7* and *ZmSKUs5.*

Supplementary File 5. FC and FP values of candidate neighboring genes.

Figure 1

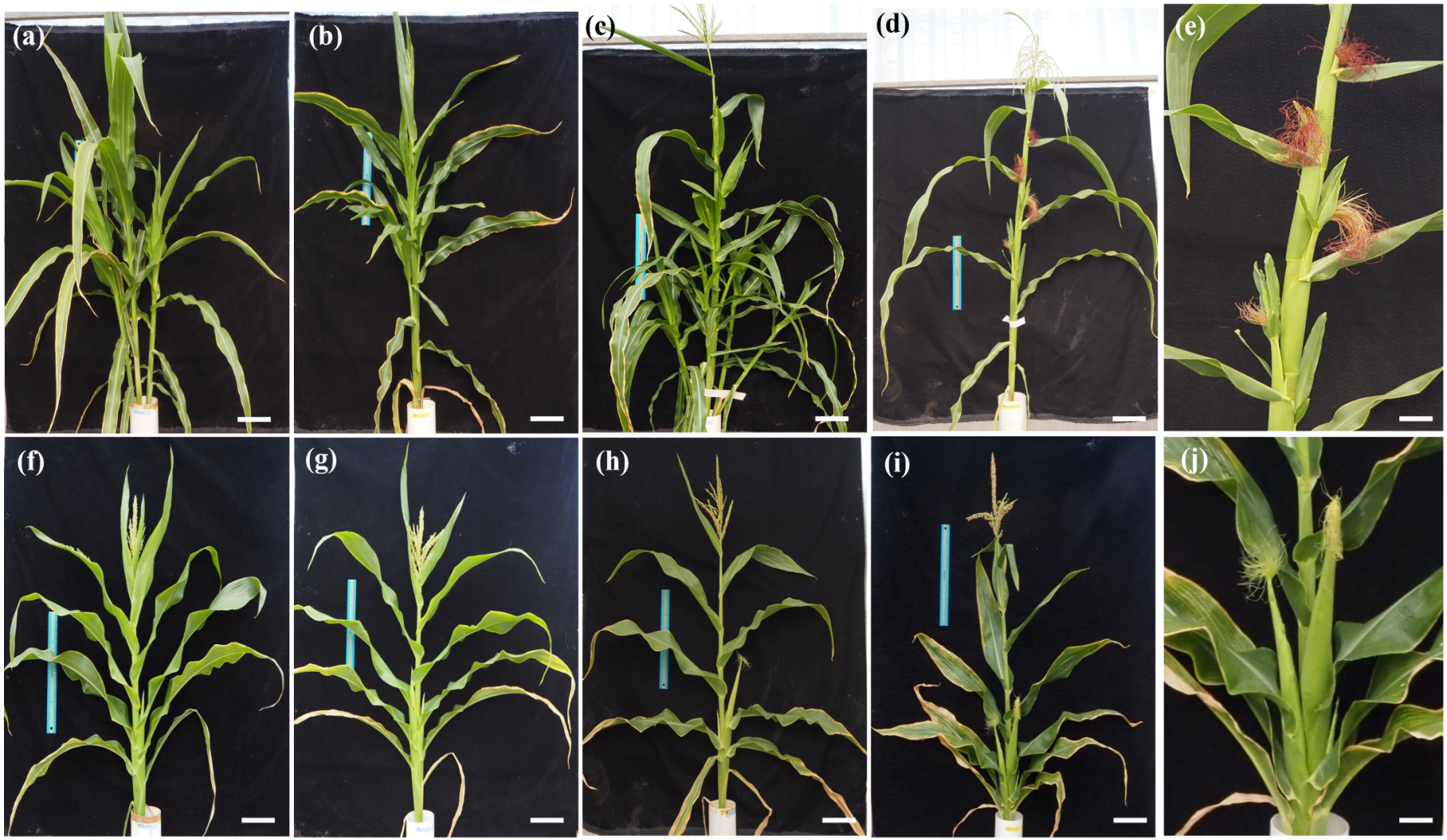

Figure 2.

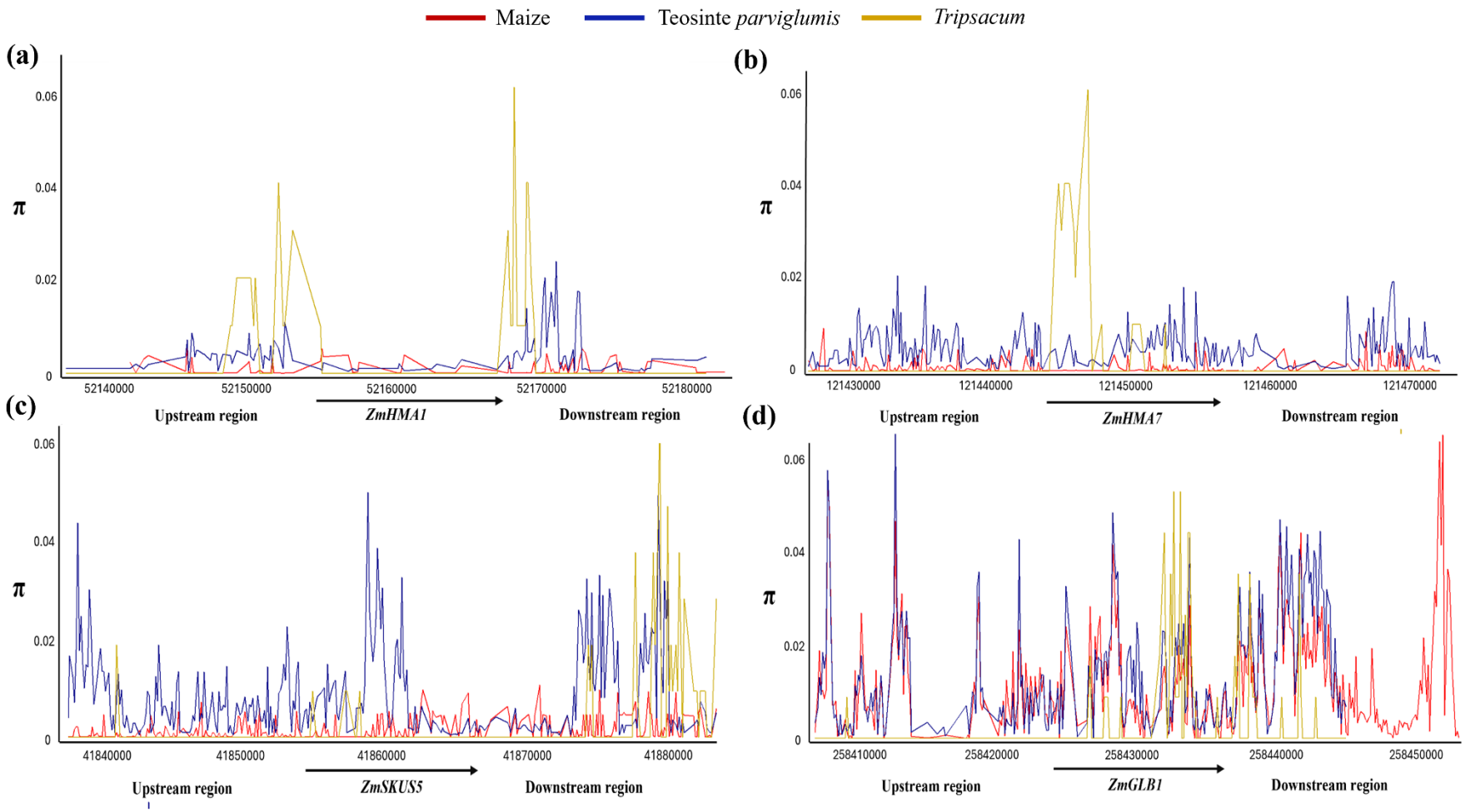
Maize
Teosinte parviglumis
Tripsacum
(a)
(b)
(c)
(d)
π
0.06
0.04
0.02
0
52140000
52150000
52160000
52170000
52180000
121430000
121440000
121450000
121460000
121470000
41840000
41850000
41860000
41870000
41880000
258410000
258420000
258430000
258440000
258450000
Upstream region
Downstream region
ZmHMA1
ZmHMA7
ZmSKUS5
ZmGLB1

Figure 3.

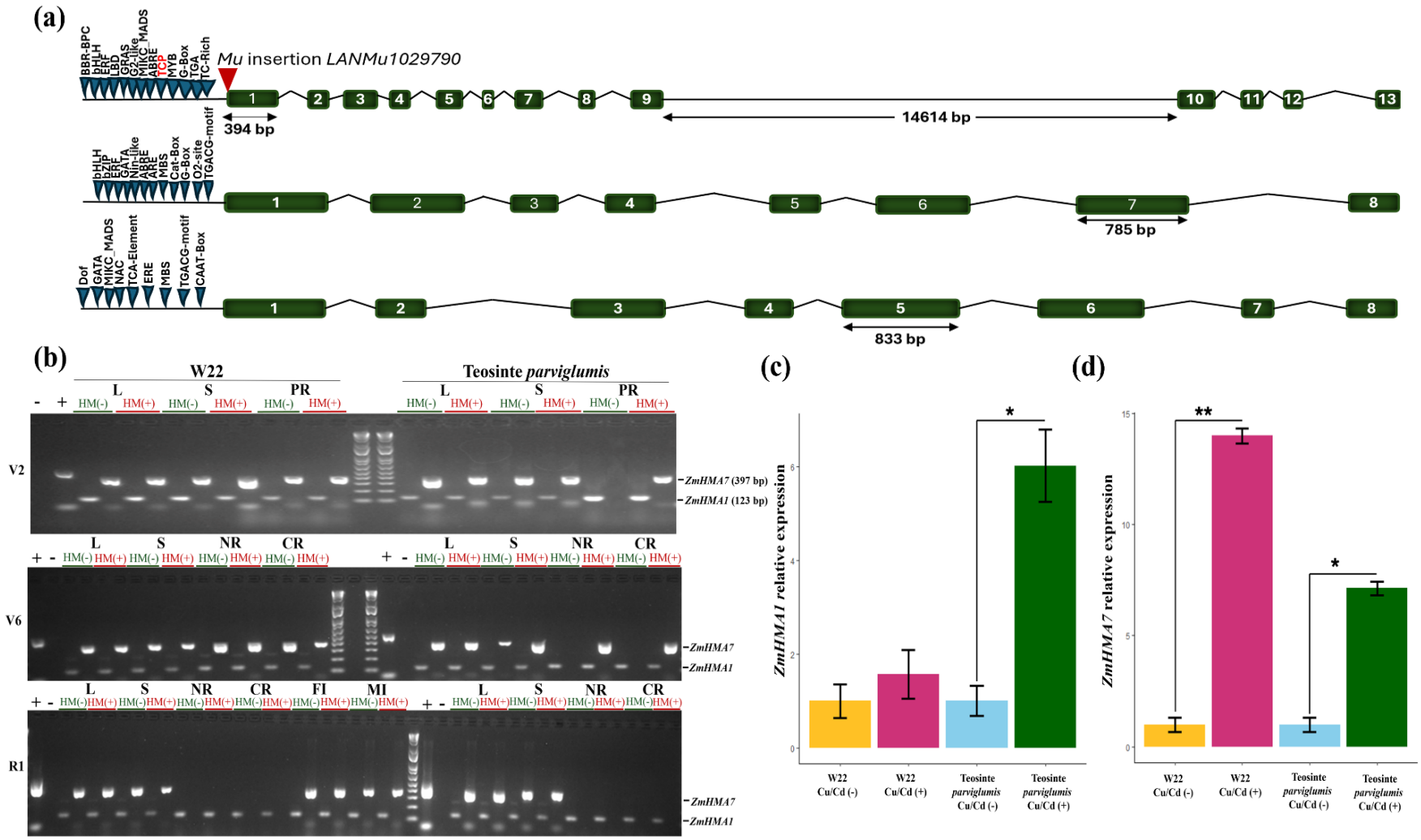
(a)
Mu insertion LANMu1029790
394 bp
14614 bp
785 bp
833 bp
(b)
W22
Teosinte parviglumis
V2
V6
R1
ZmHMA7 (397 bp)
ZmHMA1 (123 bp)
ZmHMA7
ZmHMA1
(c)
ZmHMA1 relative expression
W22 Cu/Cd (-)
W22 Cu/Cd (+)
Teosinte parviglumis Cu/Cd (-)
Teosinte parviglumis Cu/Cd (+)
(d)
ZmHMA7 relative expression

Figure 4.

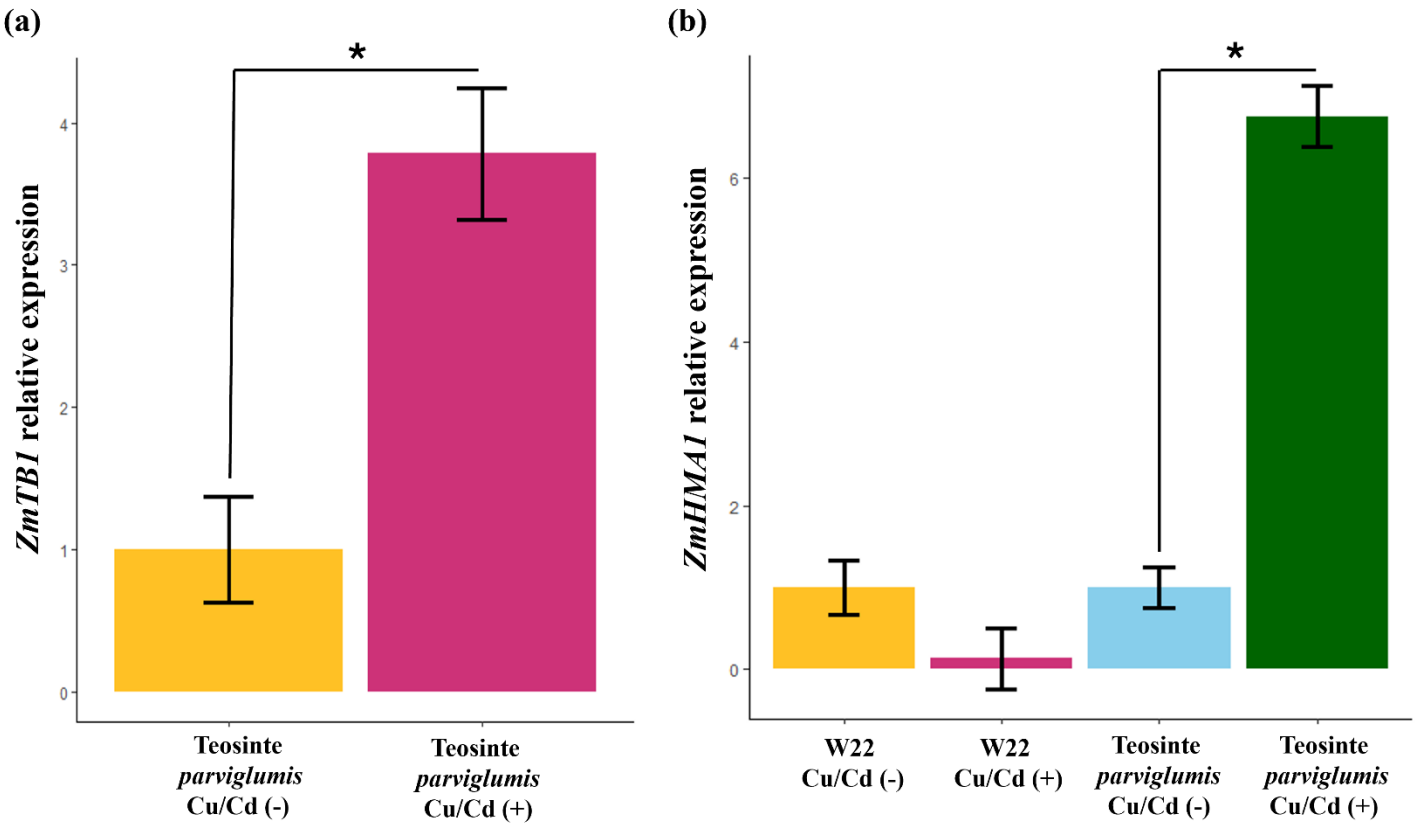
(a)
*
ZmTB1 relative expression
0
1
2
3
4
Teosinte parviglumis Cu/Cd (-)
Teosinte parviglumis Cu/Cd (+)
(b)
*
ZmHMA1 relative expression
0
2
4
6
W22 Cu/Cd (-)
W22 Cu/Cd (+)
Teosinte parviglumis Cu/Cd (-)
Teosinte parviglumis Cu/Cd (+)

Table 1. Estimation of phenotypic traits in teosinte *parviglumis* grown in absence and presence of heavy metal stress.

			Cu/Cd(-)		Cu/Cd(+)		
		Description	**Mean**	**SD**	**Mean**	**SD**	**P Value**
Aerial traits	LIL	Length of Immature Leaf (cm)	71.30	11.92	56.25	7.80	0.0570
	SB	Stem Branches	5.30	1.83	0.60	0.84	0.0002***
	DWAP	Dry Weight of Aerial Part (g)	133.49	28.28	82.72	11.67	0.7430
	NFI	Number of Female Inflorescences	1.80	0.63	3.90	1.66	0.0670
	LFI	Length of Female Inflorescences (cm)	15.40	1.35	12.50	2.12	0.0650
Root traits	NBR	Number of Brace Roots	10.60	6.13	11.60	4.55	0.1210
	LBR	Length of Brace Roots (cm)	20.00	11.49	2.88	0.66	0.0045**
	NCR	Number of Crown Roots	12.80	4.34	9.60	1.43	0.0002***
	LCR	Length of Crown Roots (cm)	60.70	16.95	62.80	14.10	0.2219
	NNR	Number of Nodal Roots	16.20	4.69	14.00	3.20	0.0039**
	LNR	Length of Nodal Roots (cm)	83.00	15.76	104.00	8.46	0.0016***

** $P<0.01$; *** $P<0.001$.

Table 2. Estimation of phenotypic traits in wild-type and *zmhma1* maize grown in absence and presence of heavy metal stress.

			Cu/Cd(-)					Cu/Cd(+)				
			W22		*zmhma1*			W22		*zmhma1*		
		Description	**Mean**	**SD**	**Mean**	**SD**	**P value**	**Mean**	**SD**	**Mean**	**SD**	**P value**
Aerial traits	NL	Number of Leaves	13.40	0.84	11.40	0.84	0.00005***	12.00	1.70	11.10	0.74	0.14194
	LML	Length of Mature Leaf (cm)	77.40	6.64	69.85	9.18	0.04930*	72.35	8.81	63.85	7.31	0.03054*
	WML	Width of Mature Leaf (cm)	6.75	1.30	9.75	1.40	0.00010***	7.20	1.42	9.95	0.86	0.00006***
	LIL	Length of Immature Leaf (cm)	59.50	6.10	48.25	6.88	0.00112**	51.90	9.97	45.35	9.43	0.14868
	WIL	Width of Immature Leaf (cm)	7.45	0.80	9.25	0.72	0.00005***	6.60	1.10	8.85	0.85	0.00007***
	HEI	Height (cm)	99.60	32.61	103.15	10.76	0.74750	82.20	34.94	125.90	18.81	0.00266**
	SD	Stem Diameter (cm)	3.24	0.52	3.02	0.51	0.34945	2.60	0.53	2.86	0.59	0.31207
	DWAP	Dry Weight of Aerial Part (g)	28.43	8.04	28.46	9.54	0.02042*	25.22	8.26	31.44	18.85	0.00156**
	NSB	Number of Spike Branches	9.00	1.63	13.40	2.32	0.00011***	7.20	3.16	13.60	1.96	0.00004***
	NFI	Number of Female Inflorescences	1.20	0.42	1.90	0.32	0.00054***	0.70	0.67	1.60	0.52	0.00357***
	WFI	Weight of Female Inflorescences (g)	40.06	14.39	69.53	11.20	0.00007***	37.75	18.83	76.06	25.04	0.00113**
Root traits	NBR	Number of Brace Roots	12.90	4.33	10.60	6.29	0.35370	16.30	4.99	9.50	6.79	0.01998*
	LBR	Length of Brace Roots (cm)	16.15	9.75	15.75	14.03	0.94179	4.00	2.04	2.67	2.01	0.15890
	NCR	Number of Crown Roots	11.30	2.11	12.10	2.42	0.44153	7.60	0.97	9.00	2.58	0.12569
	LCR	Length of Crown Roots (cm)	58.90	21.87	50.50	13.44	0.31442	48.85	11.80	44.40	20.75	0.56281
	NNR	Number of Nodal Roots	10.50	2.27	8.50	2.42	0.07262	6.70	2.79	8.00	1.56	0.21505
	LNR	Length of Nodal Roots (cm)	87.20	16.80	50.90	12.83	0.00004***	55.30	21.10	53.90	31.59	0.90850
	NSR	Number of Seminal Roots	4.10	1.45	7.30	1.16	0.00004***	6.60	1.35	8.20	1.62	0.02743*
	LSR	Length of Seminal Roots (cm)	27.70	13.38	21.33	10.31	0.24838	43.50	14.01	53.90	20.85	0.20694

* P<0.05; ** P<0.01; *** P<0.001.

25 **Appendix**
26
27 **Article title**: The influence of heavy metal stress on the evolutionary transition of
28 teosinte to maize
29 **Authors**: Jonathan Acosta-Bayona, Miguel Vallebueno-Estrada, and and Jean-Philippe
30 Vielle-Calzada
31

Figure S1. Cumulative plot of QTL detected in a region of chromosome five that includes *ZmSKUs5* and *ZmHMA1* (modified from Lemmon and Doebley, 2024).

Figure S2. Comparison of chromosome 5 nucleotide variability between maize landraces and teosinte *parviglumis*.

Figure S3. Expression of *ZmHMA1* in wild-type and homozygous *zmhma1* maize individuals.

Figure S4. Speculative model illustrating the influence of heavy metal stress on the evolutionary transition of teosinte *parviglumis* to maize.

Table S1. Additional estimation of phenotypic traits in teosinte *parviglumis* grown in absence or presence of heavy metal stress.

Table S2. Additional estimation of phenotypic traits in wild-type and *zmhma1* maize grown in absence or presence of heavy metal stress.

Table S3. Full comparison of phenotypic values for wild-type W22, *zmhma1*, and teosinte *parviglumis* individuals grown under absence or presence of heavy metal stress

Table S4. Nucleotide variability across the *ZmSKUS5, ZmHMA*1 and *ZmHMA7* locus; and their upstream and downstream neighboring genes in maize landraces, maize improved lines, and teosinte *parviglumi*s accessions included in HapMap3.

Table S5. Collection of primers used in this study.

Table S6. Maize landrace accessions used in the genetic diversity analysis chr5.

Table S7. Teosinte *parviglumis* accessions used in the genetic diversity analysis chr5.

Table S8. List of domestication genes present on chr5 as defined by Hufford et al. 2012

Supplementary Files.

Supplementary File 1. List of domestication genes present on chr5 as defined by Hufford et al. 2012

Supplementary File 2. FC and FP values for all domestication genes present in chr5.

Supplementary File 3. FC and FP values of neutral regions included in chr5.

Supplementary File 4. FC and FP values of candidate genes *ZmHMA1*, *ZmHMA7* and *ZmSKUs5.*

Supplementary File 5. FC and FP values of *ZmHMA1*, *ZmHMA7* and *ZmSKUs5* neighboring genes

Figure S1. Cumulative plot of QTL detected in a region of chromosome five that includes *ZmSKUs5* and *ZmHMA1* (modified from Lemmon and Doebley, 2024). Molecular marker positions and gene location of *ZmSKUs5* and *ZmHMA1* are in centimorgans. Abbreviated QTLs are in the left margin. The 1.5-LOD support intervals for QTLs are in black horizontal bars and peak LOD scores in vertical lines. Hatched bars indicate interacting QTLs. Gray vertical shadings indicate the presence of a QTL cluster.

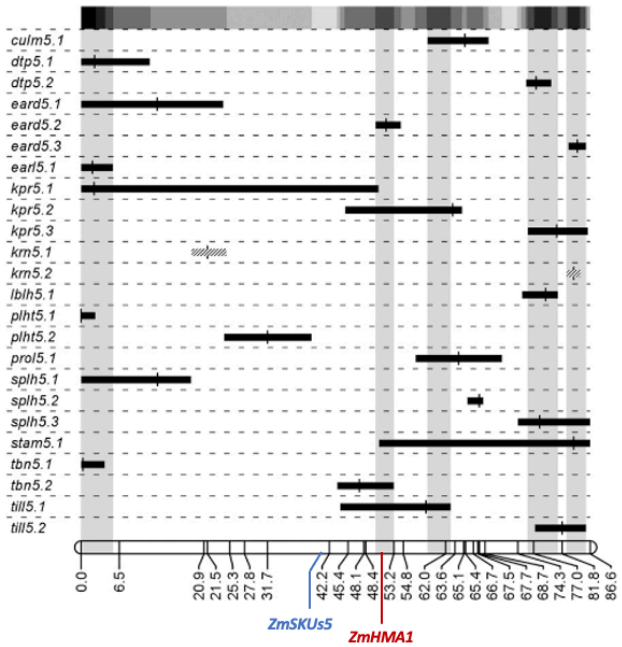

culm: diameter of culm
dtp: days to pollen shed
eard: ear diameter
earl: ear length
kpr: kernels per rank
krn: kernel row number
lblh: primary lateral branch legth
plht: plant height
prol: prolificacy, ears on lateral branch
splh: spikelet length
stam: % of staminate spikelets
tbn: tassel branch number
till: tillering index

Fig. S2 Comparison of chromosome 5 nucleotide variability between maize landraces and teosinte *parviglumis*. Violin plots represent all neutral regions comprised chromosome 5 (blue), domestication genes previously reported in chromosome 5 (Hufford et al., 2012; green), the three candidate genes in this study (white), and their six neighboring genes (red). ANOVA-Tukey tests are represented by letters.

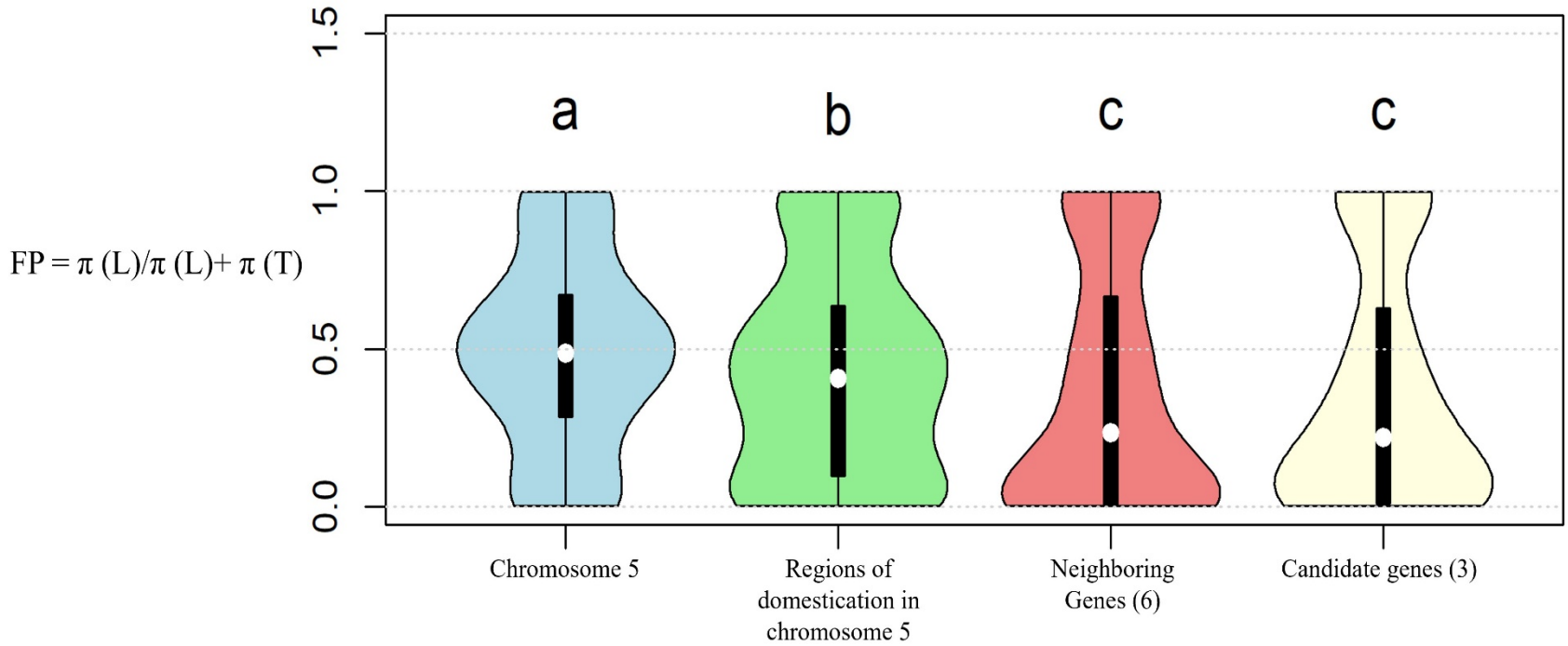

Fig. S3 Expression of *ZmHMA1* in wild-type and homozygous *zmhma1* maize individuals. A fragment of *ZmHMA1* was the target of RT-PCR amplification in fourteen W22 wild-type and fourteen *zmhma1* homozygous individuals. *ZmCDK* was used as a positive control in Wild-type individual number 1. A reaction without cDNA addition was used as a negative control. Corresponding primers are presented in Table S7.

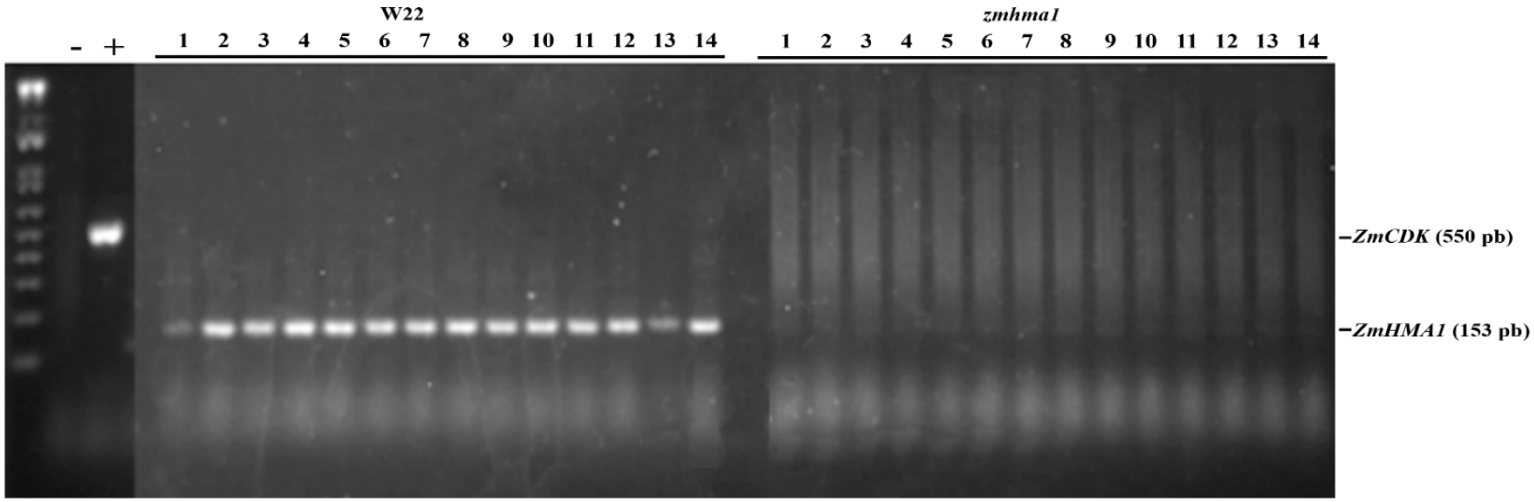

Figure S4. Model illustrating the influence of heavy metal stress on the evolutionary transition of teosinte *parviglumis* to maize.

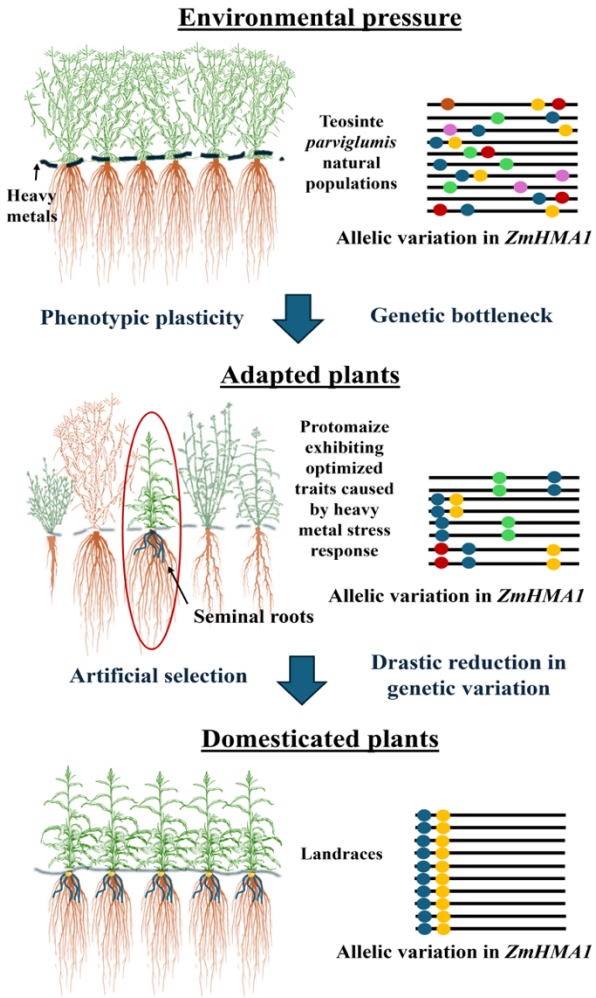

Table S1 **Additional estimation of phenotypic traits in teosinte**

***parviglumis* grown in absence or presence of heavy metal stress**. * P<0.05; ** P<0.01.

			Cu/Cd(-)		Cu/Cd(+)		
		Description	**Mean**	**SD**	**Mean**	**SD**	**P Value**
Aerial traits	NL	Number of Leaves	11.00	2.21	11.40	1.71	0.0360*
	LML	Length of Mature Leaf	84.50	4.74	81.30	8.33	0.1662
	WML	Width of Mature Leaf	5.45	0.50	6.00	1.25	0.4685
	WIL	Width of Immature Leaf	7.10	1.02	6.90	0.61	0.0650
	NN	Number of Nodes	9.30	0.95	9.80	1.55	0.0770
	HEI	Height	127.30	27.33	134.56	18.51	0.2648
	SD	Stem Diameter	2.94	0.66	3.12	0.46	0.0130**
	FWAP	Fresh Weight of Aerial Part	667.04	141.02	358.94	49.84	0.7397
	NSB	Number of Spike Branches	22.10	4.75	24.70	4.90	0.1323
	LLBS	Length of Longest Branch in Spike	21.25	4.57	20.80	5.95	0.3917
Root traits	TRL	Total Root Length	105.10	7.10	94.34	44.47	0.3021
	FWR	Fresh Weight of Complete Root System	244.60	101.99	225.70	40.05	0.0892
	DWR	Dry Weight of Complete Root System	34.21	14.29	31.84	3.57	0.0892

Table S2 Additional estimation of phenotypic traits in wild-type and *zmhma1* maize grown in absence or presence of heavy metal

stress.

			Cu/Cd(-)					Cu/Cd(+)				
			W22		*zmhma1*			W22		*zmhma1*		
		Description	**Mean**	**SD**	**Mean**	**SD**	**P value**	**Mean**	**SD**	**Mean**	**SD**	**P value**
Aerial traits	NN	Number of Nodes	11.00	2.36	10.50	1.35	0.56800	9.10	2.18	10.10	1.52	0.25038
	FWAP	Fresh Weight of Aerial Part	242.56	105.73	218.93	73.36	0.56867	226.39	108.55	318.78	145.03	0.12420
	LLBS	Length of Longest Branch in Spike	21.60	1.66	17.85	4.59	0.02596*	20.45	3.74	15.75	6.99	0.07720
	LFI	Length of Female Inflorescences	24.20	2.97	24.10	3.38	0.94479	21.50	3.17	25.50	4.60	0.03618*
Root traits	TRL	Total Root Length	91.90	17.12	72.29	9.51	0.00535**	83.98	16.19	82.33	17.27	0.82821
	FWR	Fresh Weight of Complete Root System	162.20	76.45	78.76	26.24	0.00431**	104.14	47.28	79.85	31.95	0.19497
	DWR	Dry Weight of Complete Root System	6.81	3.21	5.51	1.84	0.28136	4.37	1.98	5.59	2.24	0.21342

P<0.05; ** P<0.01

Table S3 Full comparison of phenotypic values for wild-type W22, *zmhma1*, and teosinte *parviglumis* individuals grown under

absence or presence of heavy metal stress.

			W22				*zmhma1*				Teosinte *parviglumis*			
			Cu/Cd(-)		Cu/Cd(+)		Cu/Cd(-)		Cu/Cd(+)		Cu/Cd(-)		Cu/Cd(+)	
		Description	**Mean**	**SD**	**Mean**	**SD**	**Mean**	**SD**	**Mean**	**SD**	**Mean**	**SD**	**Mean**	**SD**
Aerial traits	NL	Number of Leaves	13.40	0.84	12.00	1.70	11.40	0.84	11.10	0.74	11.00	2.21	11.40	1.71
	LML	Length of Mature Leaf	77.40	6.64	72.35	8.81	69.85	9.18	63.85	7.31	84.50	4.74	81.30	8.33
	WML	Width of Mature Leaf	6.75	1.30	7.20	1.42	9.75	1.40	9.95	0.86	5.45	0.50	6.00	1.25
	LIL	Length of Immature Leaf	59.50	6.10	51.90	9.97	48.25	6.88	45.35	9.43	71.30	11.92	56.25	7.80
	WIL	Width of Immature Leaf	7.45	0.80	6.60	1.10	9.25	0.72	8.85	0.85	7.10	1.02	6.90	0.61
	NN	Number of Nodes	11.00	2.36	9.10	2.18	10.50	1.35	10.10	1.52	9.30	0.95	9.80	1.55
	HEI	Height	99.60	32.61	82.20	34.94	103.15	10.76	125.90	18.81	127.30	27.33	134.56	18.51
	SD	Stem Diameter	3.24	0.52	2.60	0.53	3.02	0.51	2.86	0.59	2.94	0.66	3.12	0.46
	SB	Stem Branches	ND	ND	ND	ND	ND	ND	ND	ND	5.30	1.83	0.60	0.84
	FWAP	Fresh Weight of Aerial Part	242.56	105.73	226.39	108.55	218.93	73.36	318.78	145.03	667.04	141.02	358.94	49.84
	DWAP	Dry Weight of Aerial Part	18.43	8.04	17.22	8.26	28.46	9.54	41.44	18.85	133.49	28.28	82.72	11.67
	NSB	Number of Spike Branches	9.00	1.63	7.20	3.16	13.40	2.32	13.60	1.96	22.10	4.75	24.70	4.90
	LLBS	Length of Longest Branch in Spike	21.60	1.66	20.45	3.74	17.85	4.59	15.75	6.99	21.25	4.57	20.80	5.95
	NFI	Number of Female Inflorescences	1.20	0.42	0.70	0.67	1.90	0.32	1.60	0.52	1.80	0.63	3.90	1.66
	LFI	Length of Female Inflorescences	24.20	2.97	21.50	3.17	24.10	3.38	25.50	4.60	15.40	1.35	12.50	2.12
	WFI	Weight of Female Inflorescences	40.06	14.39	37.75	18.83	69.53	11.20	76.06	25.04	1.29	0.74	1.29	0.56
Root traits	NBR	Number of Brace Roots	12.90	4.33	16.30	4.99	10.60	6.29	9.50	6.79	10.60	6.13	11.60	4.55
	LBR	Length of Brace Roots	16.15	9.75	4.00	2.04	15.75	14.03	2.67	2.01	20.00	11.49	2.88	0.66
	NCR	Number of Crown Roots	11.30	2.11	7.60	0.97	12.10	2.42	9.00	2.58	12.80	4.34	9.60	1.43
	LCR	Length of Crown Roots	58.90	21.87	48.85	11.80	50.50	13.44	44.40	20.75	60.70	16.95	62.80	14.10
	NNR	Number of Nodal Roots	10.50	2.27	6.70	2.79	8.50	2.42	8.00	1.56	16.20	4.69	14.00	3.20
	LNR	Length of Nodal Roots	87.20	16.80	55.30	21.10	50.90	12.83	53.90	31.59	83.00	15.76	104.00	8.46
	NSR	Number of Seminal Roots	4.10	1.45	6.60	1.35	7.30	1.16	8.20	1.62	ND	ND	ND	ND
	LSR	Length of Seminal Roots	27.70	13.38	43.50	14.01	21.33	10.31	53.90	20.85	ND	ND	ND	ND
	TRL	Total Root Length	91.90	17.12	83.98	16.19	72.29	9.51	82.33	17.27	105.10	7.10	94.34	44.47
	FWR	Fresh Weight of Complete Root System	162.20	76.45	104.14	47.28	78.76	26.24	79.85	31.95	244.60	101.99	225.70	40.05
	DWR	Dry Weight of Complete Root System	6.81	3.21	4.37	1.98	5.51	1.84	5.59	2.24	34.21	14.29	31.84	3.57

Table S4 Nucleotide variability across the *ZmSKUS5, ZmHMA*1 and *ZmHMA7* locus; and their upstream and downstream neighboring genes in maize landraces, maize improved lines, and teosinte *parviglumi*s accessions included in HapMap3.

			Upstream(30Kb)			Coding Region			Downstream(30Kb)		
Gene ID	GeneLength(Kp)	DistanceOfGene(Kp)	π(Maize)	π(Teosinte)	**πM/πT**	π(Maize)	π(Teosinte)	**πM/πT**	π(Maize)	π(Teosinte)	**πM/πT**
GRMZM2G375607[a]	0.17	37.3	0.00105	0.000675	1.5556	0.037894	0.0304718	1.2436	0.00041	0.00064	0.6406
GRMZM2G076985[b]	4.17	-	0.011884529	0.017749593	0.669566282	0.000437979	0.007541557	0.058075436	0.002030405	0.006264344	0.324120984
GRMZM2G014508[c]	22.8	97.2	0.00844561	0.005282053	1.598925645	0.037149063	0.011257665	3.299890491	0.002433718	0.017648094	0.13790262
GRMZM2G367857[d]	8.72	25.7	0.005243813	0.006394847	0.820006014	0.008991137	0.011367691	0.790937843	0.002425106	0.006884682	0.352246578
GRMZM2G067853[e]	21.6	-	0.01329488	0.01772011	0.750270738	0.005748	0.0010578	5.433919455	0.00096874	0.0024874	0.389458873
GRMZM2G067883[f]	0.78	24.9	0.005048118	0.007825611	0.645076531	0.00119172	0.000102418	11.63584526	0.003030221	0.00681471	0.444658834
GRMZM2G374375[g]	1.84	228.6	0.0007481	0.000974	0.768069815	0.00974	0.01495	0.651505017	0.00054	0.00948	0.056962025
GRMZM2G029951[h]	4.5	-	0.000678	0.010784	0.06287092	0.00015	0.00148	0.101351351	0.00066	0.00454	0.145374449
GRMZM2G701784[i]	0.54	56	0.0005974	0.009748	0.061284366	0.00074	0.01784	0.041479821	0.00017	0.00009	1.888888889
GRMZM2G067919[j]	2.4	-	0.00611	0.00809	0.755253399	0.01035	0.01058	0.97826087	0.01417	0.01254	1.129984051

[a]Uncharacterized gene; [b]*ZmSKUS5* (Multicopper oxidase); [c]*ZmDds_sub1* (Decaprenyl-diphosphate synthase subunit 1); [d]Uncharacterized gene; [e]*ZmHMA1;* [f]Uncharacterized gene; [g]*Zmpgl20* (Exopolygalacturonase-like); [h]*ZmHMA7*; [i]Uncharacterized gene; [j]*ZmGLB1* (Globulin1)

Table S5. Collection of primers used in this study.

Primer Name	Gene ID	Forward	Reverse
*ZmHMA1*_PCR/qPCR	GRMZM2G067853_T02	TGAACACTCCGACATGGTCC	GGTGTAGCTTGAGGGAGAGC
*ZmHMA7*_PCR/qPCR	GRMZM2G029951_T01	ATCTCCTGCGCTTCTTGTGC	CCTCTGGCCTGTACTGAACC
*ZmTb1*_qPCR	Zm00001eb054440	CCCATGGACTTACCGCTTTA	GGGAGCATGGGTAGCAGTAG
*ZmCDK*_PCR	Zm00001eb215750_T001	GGAAGGTATGCACAGGACAGAT	TTCAGCACAATCTTGGCAAAAC
*ZmCDK*_qPCR	Zm00001eb215750_T001	CCGTCATCGCCTCACGAAGAG	AGAGCCTGCCTTACGGAATTGG
ZmHMA1 genotyping	GRMZM2G067853_T02	GACGACACAAGCCAAAACAG	AGGGAGATGCAGCAGAGGT

Table S6. Maize landrace accessions used in the genetic diversity analysis of chr5.

1	BKN009
2	BKN010
3	BKN011
4	BKN014
5	BKN015
6	BKN016
7	BKN017
8	BKN018
9	BKN019
10	BKN020
11	BKN022
12	BKN023
13	BKN025
14	BKN026
15	BKN027
16	BKN029
17	BKN030
18	BKN031
19	BKN032
20	BKN033
21	BKN034
22	BKN035
23	BKN040

Table S7. Teosinte *parviglumis* accessions used in the genetic diversity analysis of chr5.

1	TIL01
2	TIL01-JD
3	TIL02
4	TIL03
5	TIL04-TIP285
6	TIL04-TIP454
7	TIL05
8	TIL06-TIP260
9	TIL06-TIP496
10	TIL07
11	TIL09
12	TIL10
13	TIL11
14	TIL12
15	TIL14-TIP498
16	TIL15
17	TIL16
18	TIL17